UNIVERSIDADE FEDERAL DE SANTA CATARINA
CENTRO TECNOLÓGICO
DEPARTAMENTO DE ENGENHARIA QUÍMICA E ENGENHARIA DE ALIMENTOS

EMILY MARQUES DOS REIS

FUNCIONALIZAÇÃO DE HIDROGÉIS DE NANOCELULOSE BACTERIANA PARA MIMETIZAÇÃO DE MICROAMBIENTE TUMORAL

Florianópolis – SC
Julho, 2016

EMILY MARQUES DOS REIS

FUNCIONALIZAÇÃO DE HIDROGÉIS DE NANOCELULOSE BACTERIANA PARA MIMETIZAÇÃO DE MICROAMBIENTE TUMORAL

Dissertação submetida ao Programa de Pós-Graduação em Engenharia Química da Universidade Federal de Santa Catarina como requisito parcial para a obtenção do título de Mestre em Engenharia Química

Orientador:
Prof. Dr. Luismar Marques Porto

Coorientadora:
Drª. Fernanda Vieira Berti

Emily Marques dos Reis

Ficha de identificação da obra elaborada pelo autor através do Programa de Geração Automática da Biblioteca Universitária da UFSC

Reis, Emily Marques dos
Funcionalização de Hidrogéis de Nanocelulose Bacteriana para Mimetização de Microambiente Tumoral / Emily Marques dos Reis ; orientador: Luismar Marques Porto , coorientadora, Fernanda Vieira Berti – Florianópolis, SC, 2016.
127p.

Dissertação (mestrado) – Universidade Federal de Santa Catarina, Centro Tecnológico. Programa de Pós-graduação em Engenharia Química.

Inclui referências

1. Engenharia Química. 2. Nanocelulose bacteriana. 3. microambiente tumoral. 4. HUVECs. 5. SK-MEL-28. I. Porto, Luismar Marques. II. Berti , Fernanda Vieira. III. Universidade Federal de Santa Catarina. Programa de Pós-graduação em Engenharia Química. IV. Título.

FUNCIONALIZAÇÃO DE HIDROGÉIS DE NANOCELULOSE BACTERIANA PARA MIMETIZAÇÃO DE MICROAMBIENTE TUMORAL

Por

Emily Marques dos Reis

Dissertação julgada para obtenção do título de Mestre em Engenharia Química, área de Concentração de Desenvolvimento de Processos Químicos e Biotecnológicos e aprovada em sua forma final pelo Programa de Pós-Graduação em Engenharia Química da Universidade Federal de Santa Catarina.

Prof. Dr. Luismar Marques Porto
Orientador

Drª. Fernanda Vieira Berti
Coorientadora

Banca Examinadora:

Prof. Dr. Agenor Furigo Júnior
Membro Interno

Prof. Dr. Carlos Renato Rambo
Membro Externo

Prof. Dr. Paulo Fernando Dias
Membro Externo

AGRADECIMENTOS

Em primeiro lugar a Deus, por todas as conquistas alcançadas.

Ao Professor Luismar Marques Porto pela orientação e ensinamentos.

À Drª Fernanda Vieira Berti, pela orientação, ensinamentos, dedicação, carinho e por sempre acreditar neste trabalho.

A todo o grupo do Laboratório de Tecnologias Integradas (InteLab).

À doutoranda Karina Cesca, obrigada por me ajudar desde o início do mestrado, sempre me incentivando e acreditando nas minhas ideias.

Ao doutorando Guilherme Colla, obrigada por sempre estar disposto a me ajudar, você contribuiu para a realização deste trabalho.

Ao mestrando Maikon Kelbert, obrigada por sempre estar presente e disposto a me ajudar.

Às alunas de iniciação científica Tuane Antonio e a Ana Carolina pelo auxilio nos experimentos de cultura celular.

Ao Dr. Charles Kondageski, pela esterilização das amostras.

Ao meu amigo Fabrício de Mello, pela ajuda prestada.

Ao Laboratório Central de Microscopia Eletrônica (LCME-UFSC) pelas análises de microscopia confocal e mcroscopia eletrônica de varredura.

Ao meu namorado, André Vinícius, pelo apoio, ajuda, carinho e amor durante toda a realização deste trabalho.

À toda minha família em especial aos meus pais, Geziel dos Reis e Angela Marques dos Reis pelas orientações e apoio constante que me permitiram crescer como pessoa e a chegar nesse momento.

Ao CNPq, à CAPES e à FINEP, pelo apoio financeiro

FUNCIONALIZAÇÃO DE HIDROGÉIS DE NANOCELULOSE BACTERIANA PARA MIMETIZAÇÃO DE MICROAMBIENTE TUMORAL

RESUMO

O desenvolvimento de um sistema adequado de cultura de células em três dimensões (3D) para a seleção de fármacos anticâncer continua a ser uma necessidade não atendida. Um modelo 3D do microambiente tumoral simples, rápido, reprodutível e de baixo custo ainda não foi desenvolvido. Alterações do microambiente são fundamentais para a metástase e culturas em 3D podem ser utilizadas para estudar os mecanismos e efeitos que estas alterações causam na sinalização de células tumorais. O objetivo deste trabalho foi desenvolver modelos de bioengenharia para o estudo do comportamento de células endoteliais e células de melanoma que possam servir como matrizes para o rastreio de potenciais fármacos antitumorais. Primeiramente, hidrogéis de nanocelulose bacteriana (BNC) foram oxidados com HNO_3/H_3PO_4-$NaNO_2$, seguido por derivatização com um agente de acoplamento e finalmente, a heparina ou IKVAV foram imobilizadas sobre os hidrogéis através de ligações covalentes, funcionalizando assim esses biomateriais. O sucesso das imobilizações foi confirmado por técnicas de caracterização de materiais. As células endoteliais de veia umbilical humana (HUVECs) foram semeadas nas superfícies inferior e superior dos hidrogéis BNC e BNC-HEP e o comportamento celular foi observado. A superfície inferior do BNC-HEP é capaz de suportar a adesão celular, proliferação e induzir tubulogênese. Células de melanoma humano (SK-MEL-28) quando semeadas sobre as superfícies superior e inferior dos hidrogéis BNC e BNC-IKVAV adquiriram diferentes plasticidades tumorais como, por exemplo, o mimetismo vasculogênico. Os resultados aqui apresentados indicam que o comportamento celular pode ser controlado por interações simples com grupos funcionais em vez de biomoléculas solúveis ou materiais complexos, o que tornaria a produção de materiais para o estudo da angiogênese, mecanismos de invasão celular e mimetismo vasculogênico, mais baratos e facilmente controlados. Os biomateriais aqui desenvolvidos e estudados podem ser utilizados para a elucidação de diversos mecanismos celulares que levam à metástase tumoral. Assim, fármacos poderão ser testados contra diversas plasticidades celulares, visando o tratamento de câncer e de outras doenças de interesse biomédico.

Palavras-chave: Nanocelulose bacteriana; microambiente tumoral; HUVECs; SK-MEL-28; plasticidades celulares; angiogênese; mimetismo vasculogênico.

FUNCTIONALIZATION OF BACTERIAL NANOCELULOSE HYDROGELS TO MIMICKING OF TUMOR MICROENVIRONMENT

ABSTRACT

The development of a suitable system of three dimensions in cell culture (3D) for the selection of anticancer drugs remains an unmet need. A 3D model of the tumor microenvironment simple, fast, reproducible and low cost has not yet been developed. Changes in the microenvironment are fundamental to metastasis and 3D cultures can be used to study the mechanisms and effects that these changes have on the signaling of tumor cells. The aim of this study was to develop bioengineering models for the study of endothelial cell behavior and of melanoma cells that can serve as matrix for the screening of potential anti-tumor drugs. First, hydrogels bacterial nanocelulose (BNC) were oxidized with HNO_3/H_3PO_4-$NaNO_2$, followed by derivatization with a coupling agent and finally heparin or IKVAV were immobilized on hydrogels by covalent bonds. The success of immobilization was confirmed by techniques for material characterization. Endothelial cells from human umbilical vein (HUVECs) were seeded in the top and bottom surfaces of hydrogels BNC and BNC-HEP and cell behavior was observed. The bottom surface of HEP-BNC is capable of supporting cell adhesion, proliferation and induce tubulogênese. Human melanoma cells (SK-MEL-28) when seeded on the upper and lower surfaces of hydrogels BNC and BNC-IKVAV acquired different tumor plasticities as, for example, vasculogenesis mimicry. The results presented herein indicate that the cellular behavior can be controlled by simple interactions with the functional groups instead of soluble biomolecule or complex materials. Thus, the production of material for the study of angiogenesis, cell invasion mechanisms and vasculogenesis mimicry can be easily controlled. Biomaterials developed and studied here may be used for the elucidation of many cellular mechanisms that lead to tumor metastasis. Thus, drugs can be tested against various cellular plasticity, targeting the treatment of cancer and other diseases of biomedical interest.

Keywords: Bacterial nanocellulose; tumor microenvironment; HUVECs; sk-mel-28; cells plasticity; angiogenesis; vasculogenic mimicry.

.

LISTAS DE FIGURAS

Capítulo 2- Revisão bibliográfica

Capítulo 3 - *Immobilization of heparin on bacterial nanocellulose hydrogels induces human endothelial cell tubulogenesis*

LISTA DE SIGLAS E ABREVIATURAS

3D: tridimensional

2D: bidimensional

BNC: nanocelulose bacteriana

BNC-HEP: hidrogel de nanocelulose bacteriana funcionalizado com heparina

BNC-IKVAV: hidrogel de nanocelulose bacteriana funcionalizado com IKVAV

DAPI: (4'-6-diamidino-2-fenilindol)

ECM: matriz extracelular

EDC: (1-etil-3-(3-dimetilaminopropil carbodiimida)

FTIR: espectroscopia de infravermelho com transformada de Fourier

HEP: heparina

HUVECs: células endoteliais de veia umbilical humana

IKVAV: Isoleucina-Lisina-Valina-Alanina-Valina

MEC: matriz extracelular

MEV: microscopia eletrônica de varredura

MTS: [3-(4,5-dimetiltiazol-2-il)-5-(3-carboximetoxifenil)-2-(4-sulfofenil)-2H-tetrazólio].

SK-MEL-28: células de melanoma humano

SUMÁRIO

1 INTRODUÇÃO

De acordo com a Organização Mundial de Saúde (OMS) no ano de 2025 serão registrados mais de 20 milhões de novos casos de câncer (WORLD HEALTH ORGANIZATION; STEWART; WILD, 2014). A estimativa para o Brasil, referente aos anos de 2016–2017, aponta a ocorrência de cerca de 600 mil novos casos da doença (INSTITUTO NACIONAL DE CANCER JOSÉ ALENCAR GOMES DA SILVA, 2016). A proliferação secundária das células tumorais no que diz respeito à invasão de outros tecidos e órgãos é responsável pela maior parte dos óbitos de pacientes com câncer (BALTIĆ, 2006).

A plasticidade das células tumorais está relacionada ao crescimento do tumor e a proliferação destas células através de um complexo mecanismo celular, conhecido como metástase tumoral (MARTIN *et al*., 2013). Durante a metástase as células tumorais invasivas modulam o próprio citoesqueleto com o objetivo de migrar por diferentes mecanismos e proliferar invadindo outros tecidos (JOYCE; POLLARD, 2009).

Existem, ao menos duas vias de disseminação metastática uma delas dirigida por angiogênese e a outra denominada de mimetismo vasculogênico (FOLBERG; HENDRIX; MANIOTIS, 2000). Durante o aumento da massa tumoral, as células tumorais liberam moléculas sinalizadoras responsáveis pelo recrutamento de vasos sanguíneos que suprem a demanda de oxigênio e nutrientes necessários para a progressão tumoral (CARMELIET; JAIN, 2000; FOLKMAN, 1971). O recrutamento destes novos vasos sanguíneos a partir de vasos pré-existentes se dá por meio de um processo denominado angiogênese (FOLKMAN, 1971a). As células tumorais migram para o interior destes vasos sanguíneos recrutados e são conduzidas para outros órgãos onde se alojam concluindo o processo metastático (VALASTYAN; WEINBERG, 2011).

Outra via de disseminação tumoral acontece através de um mecanismo denominado mimetismo vasculogênico (MANIOTIS *et al*., 1999a). No mimetismo vasculogênico as células tumorais assumem o comportamento de células endoteliais mimetizando os tubos vasculares

em busca de oxigênio e outros nutrientes para o crescimento do tumor. Desta forma, assim que as células tumorais acessam o endotélio vascular elas migram para o interior do vaso sanguíneo e depois para outros órgãos, assim como acontece na disseminação metastática por angiogênese (FOLBERG; HENDRIX; MANIOTIS, 2000; FOLBERG; MANIOTIS, 2004).

Neste cenário, a busca de novos fármacos que possam combater os diversos mecanismos celulares que levam a metástase, se faz necessária. O desenvolvimento de um novo fármaco anticâncer custa aproximadamente 1 bilhão de dólares (LIGHT; KANTARJIAN, 2013), sendo que apenas 10% dos novos medicamentos para combater o câncer realmente tem sido eficaz, adicionando apenas algumas semanas ou meses para a vida de um paciente (HAIT, 2010). A baixa eficácia dos fármacos antitumorais é devida, principalmente, ao uso de modelos inconsistentes utilizados na realização dos testes pré-clínicos (GEVAERT, 2012).

Sem dúvida, os componentes do microambiente desempenham um papel-chave na regulação destas vias de disseminação tumoral através de metástase (BISSELL; RADISKY, 2001). Assim, existe um esforço para substituir os métodos de rastreio convencionais, atualmente realizados em plataformas bidimensionais (2D). Neste sentido, a substituição das plataformas 2D por modelos tridimensionais (3D), que mimetizam o microambiente tumoral é de extrema relevância clínica (KIMLIN; CASAGRANDE; VIRADOR, 2013a, 2013b; YAMADA; CUKIERMAN, 2007).

Devido à sua capacidade de simular a natureza da maior parte dos tecidos moles, os hidrogéis são materiais altamente atrativos para o desenvolvimento de matriz extracelular (MEC) sintética. Estas estruturas compostas de cadeias de polímeros reticulados possuem alto teor de água, fácil transporte de oxigênio, nutrientes, resíduos, bem como o transporte de fatores solúveis (NGUYEN; WEST, 2002). Além disso, os hidrogéis podem ser quimicamente modificados mimetizando a funcionalidade de moléculas sinalizadoras e direcionando o comportamento celular (DRURY; MOONEY, 2003; EL-SHERBINY; YACOUB, 2013b; VAN VLIERBERGHE; DUBRUEL; SCHACHT, 2011; ZHU; MARCHANT, 2011). Entretanto, as matrizes de 3D de

origem animal comercialmente disponíveis, apresentam composição química indefinida, o que resulta em resultados não reprodutíveis (KLEINMAN; MARTIN, 2005). Devido à necessidade de se estudar o microambiente tumoral e desenvolver novos fármacos para combater a metástase, é necessário o desenvolvimento de modelos que consigam representar o ambiente tumoral como acontece in vivo (ASGHAR *et al*., 2015; NYGA; CHEEMA; LOIZIDOU, 2011; OU; HOSSEINKHANI, 2014; YAMADA; CUKIERMAN, 2007). Esses modelos precisam ser reprodutíveis, não ter a interferência de diversas moléculas nos resultados e ser de fácil uso.

Desta forma, este trabalho propõe o desenvolvimento de duas plataformas 3D que possam ser utilizadas no rastreio de antitumorais eficientes na inibição da progressão tumoral. Dentre as plataformas desenvolvidas, a primeira baseou-se na imobilização de heparina nos hidrogéis de nanocelulose bacteriana provendo um microambiente capaz de induzir as células endoteliais a mimetizar a via metastática relacionada a angiogênese. A outra plataforma 3D desenvolvida baseou-se na imobilização de um peptídeo derivado de laminina, o IKVAV (Isoleucina-Lisina-Valina-Alanina-Valina), nos hidrogéis de nanocelulose bacteriana com o intuito de induzir as células tumorais a mimetizar a via metastática do mimetismo vasculogênico e outras plasticidades no processo de invasão celular.

1.1 OBJETIVOS

1.1.1 Objetivo geral

Funcionalizar hidrogéis de nanocelulose bacteriana para mimetizar o microambiente tumoral.

1.1.2 Objetivos específicos

- Funcionalizar hidrogéis de nanocelulose bacteriana (BNC) através da imobilização química de heparina (HEP);
- Caracterizar a microestrutura dos hidrogéis BNC-HEP;
- Analisar a citotoxicidade dos hidrogéis BNC-HEP;
- Analisar o comportamento das células de veia endotelial humana (HUVECs) quanto a adesão e proliferação nos hidrogéis BNC-HEP;
- Analisar o comportamento das HUVECs na mimetização da angiogênese quando cultivadas nos hidrogéis BNC-HEP;
- Funcionalizar hidrogéis de celulose bacteriana (BNC) através de imobilização química do peptídeo IKVAV;
- Caracterizar a microestrutura dos hidrogéis BNC-IKVAV;
- Analisar a citotoxicidade dos hidrogéis BNC-IKVAV;
- Analisar o comportamento das células de melanoma humano (SK-MEL-28) quanto a adesão, proliferação e morfologia nos hidrogéis BNC-IKVAV;
- Analisar o comportamento das células SK-MEL-28 na mimetização do mimetismo vasculogênico nos hidrogéis BNC-IKVAV.

1.2 ESTRUTURA DO TRABALHO

Essa dissertação descrive a funcionalização de hidrogéis de nanocelulose bacteriana para mimetização de microambiente tumoral. A disseraão está organizada da seguinte maneira:

- Capítulo 2 − Revisão bibliográfica sobre o câncer e os mecanismos que levam a metástase tumoral.

- Capítulo 3 – *Immobilization of heparin on bacterial nanocellulose hydrogels induces human endothelial cell tubulogenesis*, que descreve a funcionalização de hidrogéis de BNC com heparina para o desenvolvimento de uma plataforma que mimetiza o ambiente tumoral na angiogênese.
- Capítulo 4 – *A novel BNC–IKVAV platform for vasculogenic mimicry and other plasticities of human melanoma cells* que descreve a funcionalização de hidrogéis BNC com o peptídeo IKVAV para o desenvolvimento de uma plataforma que mimetiza o microambiente tumoral no processo de mimetismo vasculogênico.
- Conclusões gerais sobre o trabalho.

2 REVISÃO BIBLIOGRÁFICA

2.1 CÂNCER

O câncer pode ser definido como o crescimento anormal de células, causado por alterações na expressão de genes que conduzem a desregulação da proliferação e morte celular (HANAHAN; WEINBERG, 2011). A proliferação descontrolada de células anormais resulta na formação de uma massa tumoral. Os passos subsequentes da proliferação levam ao crescimento do tumor e, eventualmente, ao rompimento da barreira da membrana basal dos tecidos circundantes e assim, o câncer se espalha para outras partes do corpo, processo denominado de metástase (HEJMADI, 2010).

A formação da metástase é dividida em várias etapas complexas chamadas de cascata de invasão da metástase. Nesse processo de invasão celular, as células tumorais primeiramente invadem a matriz extracelular local e as camadas do estroma celular e subsequentemente, o lúmen dos vasos sanguíneos e assim são transportadas através da vasculatura para tecidos distantes (GEIGER; PEEPER, 2009; JOYCE; POLLARD, 2009). A metástase é em grande parte incurável devido à sua natureza sistêmica e a resistência das células tumorais aos agentes terapêuticos existentes. Mais de 90% da mortalidade por câncer é atribuível a metástases e não aos tumores primários (CHAFFER; WEINBERG, 2011; NGUYEN; BOS; MASSAGUÉ, 2009; WAN; PANTEL; KANG, 2013).

Massas tumorais maiores que 180 µm são capazes de recrutar novos vasos sanguíneos, devido a necessidade de alta oxigenação tecidual, no processo denominado angiogênese (FOLKMAN, 1971a). Estas células, recrutam novos vasos sanguíneos para o local do tumor, através da liberação de fatores e citocinas angiogênicas e assim por meio desses novos vasos poderá ocorrer metástase (ADAIR; MONTANI, 2010; CARMELIET; JAIN, 2000; FOLKMAN, 1971).

Em determinados tumores, o processo de angiogênese não é suficiente para suprir as necessidades do tumor. Acredita-se que por esse motivo, um mecanismo independente de angiogênese está presente em

determinadas células tumorais agressivas, o mimetismo vasculogênico (FOLBERG; HENDRIX; MANIOTIS, 2000; FOLBERG; MANIOTIS, 2004; MANIOTIS *et al*., 1999a). Este mecanismo é mediado através de plasticidade de células tumorais, que adquirem características de células endoteliais no processo de angiogênese. Assim, o mimetismo vasculogênico funciona como uma via adicional para a metástase (DÖME *et al*., 2007; FOLBERG; HENDRIX; MANIOTIS, 2000).

2.1.1 Invasão celular

O primeiro passo na metástase é a migração de células invasivas tumorais para o estroma, processo chamado de invasão tumoral. Os passos iniciais de invasão local incluem a ativação de vias de sinalização que controlam a dinâmica do citoesqueleto em células tumorais, seguido pela migração de células tumorais ativas para o tecido adjacente (FRIEDL; ALEXANDER, 2011; HULKOWER; HERBER, 2011; YAMAGUCHI; WYCKOFF; CONDEELIS, 2005). A metástase, ocorre em seguida quando as células tumorais invasoras se envolvem com vasos sanguíneos e linfáticos, penetram nas membranas basais e nas paredes endoteliais, e se disseminam através do lúmen dos vasos para colonizar órgãos distantes (GEIGER; PEEPER, 2009).

A invasão tumoral requer maior motilidade celular impulsionada pela remodelação do citoesqueleto e contatos de células com a matriz extracelular, para isso as células tumorais tem a capacidade de se adaptarem a diferentes condições ambientais, assumindo diversas morfologias (plasticidade) e tipos de migração (FRIEDL; ALEXANDER, 2011; FRIEDL, 2004).

Dois padrões principais de invasão de células tumorais têm sido descritos: a migração individual de células tumorais e a migração coletiva (FRIEDL; WOLF, 2003), conforme representado na Figura 1. As células que migram isoladamente ou em grupos podem se locomover através do modo ameboide ou mesenquimal. O modo ameboide de movimento é caracterizado pelo fenótipo redondo das células. Saliências celulares, geralmente posicionadas sobre a superfície das células, são reguladas pela dinâmica do citoesqueleto e são denominadas como bolhas (*blebs*) e geralmente estão presentes no modo de movimento

ameboide. Células ameboides são mais flexíveis e podem se espremer em pequenos espaços para se locomover, mas não são capazes de degradar a MEC ou gerar novos caminhos para o tumor (LÄMMERMANN; SIXT, 2009; WOLF *et al.*, 2003). O modo ameboide parece ser preferido em situações de stress metabólico, tais como a hipóxia, o que pode implicar que o modo ameboide é menos consumidor de energia, ou mais eficiente em comparação com o modo mesenquimal (FRIEDL, 2004). No modo mesenquimal, o fenótipo celular é caracterizado por células com corpo celular alongado e longas saliências. Essas saliências são denominadas como invapodia, e degradam a MEC por interações e contatos célula-matriz (TSAI; YANG, 2013;KHALIL; FRIEDL, 2010).

Figura 1. Células tumorais podem exibir dois modos diferentes de motilidade celular: modo mesenquimal e modo ameboide. O movimento mesenquimal requer a degradação da matriz extracelular (MEC), já as células com movimento ameboide migram de uma forma independente de integrina. Esses movimentos podem representar a migração coletiva ou isolada das células tumorais.

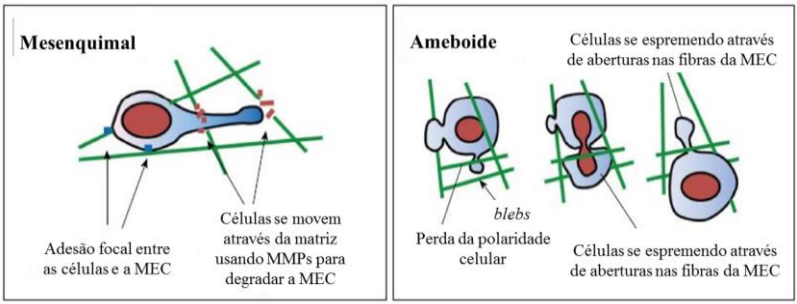

Fonte: Adaptado de (MATSUOKA; YASHIRO, 2014)

2.1.2 Angiogênese tumoral

A angiogênese é a formação de novos vasos a partir de vasos pré-existente, processo subsequente a vasculogênese, formação de novos vasos sanguíneos in situ. A angiogênese é fundamental no desenvolvimento do tumor e requer a proliferação de células endoteliais, a migração de células através da MEC e interações célula-célula

(FOLKMAN, 1971). A Figura 2 representa o processo de angiogênese tumoral.

Uma cascata de eventos deve acontecer para que a angiogênese ocorra, incluindo: liberação de fatores de crescimento pelas células tumorais, degradação da membrana basal, a ativação de células endoteliais (células *tip*), proliferação de células adjacentes (células *stalk*) e a formação de brotos de sólidos que formam o lúmen (tubulogênese) (HEJMADI, 2010).

Primeiramente, as células de tumor expressam fatores pró-angiogênicos, tais como o fator de crescimento endotelial vascular (VEGF), que se difundem para os tecidos circundantes e ligam-se a receptores nas células endoteliais dos vasos sanguíneos pré-existentes, levando à ativação das células (células *tip*). Essas interações entre as células endoteliais e células tumorais levam à secreção e ativação de várias enzimas proteolíticas, tais como metaloproteinases de matriz (MMPs), que degradam a membrana basal e a matriz extracelular. A degradação da membrana basal permite que as células *tip* migrem para o tumor. Células *tip* são células alongadas e caracterizadas pela presença de longos filamentos em uma de suas extremidades, chamadas de filapódio. Células *stalk*, células adjacentes à células *tip*, começam a proliferar e a seguir as células *tip*. Este processo resulta na formação de um broto capilar. As células *tip* não se dividem, já as células *stalk* proliferam, alongam o broto capilar e formam o lúmen. Esse processo de formação do lúmen é denominado tubulogênese. Para formar um loop (o lúmen formado na tubulogênese se dobra formando um laço), filapódio de células *tip* de diferentes brotos se conectam e estabelecem uma rede de vasos (DAVIS; SAUNDERS, 2006; DE SMET et al., 2009; SAMOLOV et al., 2005; STEEN et al., 1998). A Figura 3 mostra algumas das estruturas celulares presentes na angiogênese.

Figura 2. Etapas sequenciais da angiogênese tumoral. (1) O tumor dormente no começa a secretar fatores de crescimento angiogênicos. (2) Após as células endoteliais dos vasos circundantes são ativadas, começam a migrar e proliferam para o tumor. Uma célula tip guia a formação do broto vascular. (3) O novo broto forma um lúmen e o tumor é ligado a vasculatura, garantindo assim o crescimento e metástase do tumor (VAN HORSSEN; TEN HAGEN; EGGERMONT, 2006).

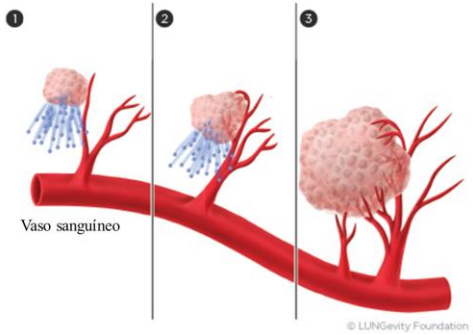

Fonte: Adaptado de (VAN HORSSEN; TEN HAGEN; EGGERMONT, 2006).

Figura 3. Comportamento e estruturas celulares presentes no processo de angiogênese.

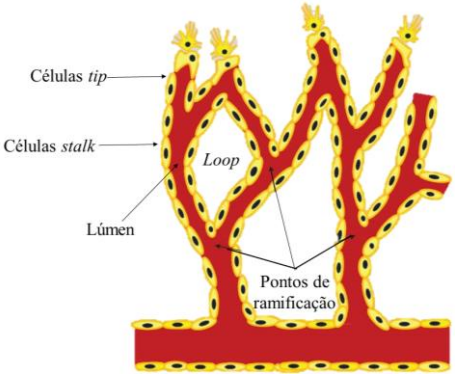

Fonte: Adaptado de (WOOD; KAMM; ASADA, 2011)

2.1.3 Mimetismo vasculogênico

O mimetismo vasculogênico foi introduzido em 1999 e descreveu a capacidade única de células de melanoma em formar canais, semelhantes a vasos, condutores de fluidos (MANIOTIS *et al*., 1999). O termo mimetismo vasculogênico é utilizado porque os canais não se formam a partir de vasos pré-existentes, apesar deles distribuírem plasma e conterem células vermelhas do sangue, mas possuem a capacidade em imitar a função dos vasos. Assim, o processo de mimetismo vasculogênico é a formação de canais, semelhantes a vasos, por células tumorais agressivas (HENDRIX *et al*., 2003). A Figura 4 mostra o suprimento do tumor através da angiogênese e do mimetismo vasculogênico.

As funções do mimetismo vasculogênico in vivo são de perfusão vascular, transporte de fluidos e nutrição, todos os requisitos críticos em estágios iniciais do crescimento tumoral. A caracterização morfológica das redes de mimetismo vasculogênico revelaram que estas são ricas em laminina extravasculares circundantes a esferoides de células tumorais (FOLBERG; HENDRIX; MANIOTIS, 2000; FOLBERG; MANIOTIS, 2004).

Acreditasse que o processo de mimetismo vasculogênico ocorra porque o crescimento tumoral, muitas vezes, pode não ser totalmente suportado pelo processo de angiogênese (QIAO *et al*., 2015). Entretanto o mecanismo do mimetismo vasculogênico não é totalmente elucidado (LARSON *et al*., 2014). Mimetismo vasculogênico também foi relatado em tumores malignos não-melanoma tais como câncer da mama (SHIRAKAWA *et al*., 2001), de ovário (SOOD *et al*., 2001),sarcoma de Ewing (VAN DER SCHAFT *et al*., 2005) e pulmão *(*PASSALIDOU *et al*., 2002). A ocorrência de mimetismo vasculogênico é relativamente rara dentro tumores, mas sua presença está relacionada ao aumento do risco de metástase e portanto, má evolução clínica (PAULIS *et al*., 2010).

Figura 4. Ação da angiogênese e mimetismo vasculogênico no tumor. Na angiogênese, células tumorais secretam fatores angiogênicos que induzem a formação de vasos até o tumor, para suprir suas necessidades. No mimetismo vasculogênico, as próprias células tumorais adquirem características de células endoteliais e formam tubos, semelhantes a vasos.

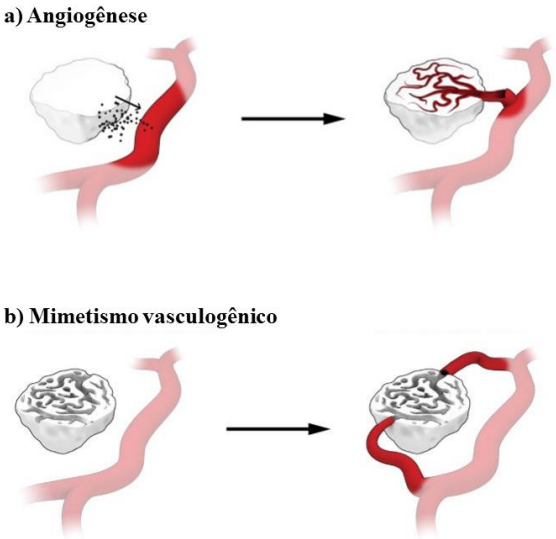

Fonte: Adaptado de (MITCH LESLIE, 2016).

2.2 TRIAGEM DE FÁRMACOS ANTICANCERTRIAGEM DE FÁRMACOS ANTICÂNCER

O desenvolvimento de fármacos anticâncer envolve testes in vitro seguido por avaliação da eficácia desses medicamentos em ensaios clínicos (LIGHT; KANTARJIAN, 2013). A falta de bons modelos pré-clínicos tem dificultado a descoberta de medicamentos anticâncer e sua implementação. Para enfrentar esses desafios, sistemas de cultura 3D são cada vez mais aplicadas no estudo da biologia do tumor (DEBNATH; BRUGGE, 2005).

Em metástase, as células tumorais invasivas precisam mudar sua organização do citoesqueleto e alterar contatos com matriz extracelular. Investigar como estas plasticidades contribuem com metástase e a migração no processo de invasão é uma maneira de desenvolver fármacos para combater a metástase (FRIEDL; ALEXANDER, 2011).

Ao longo dos últimos anos, a terapia antiangiogênica tem sido uma estratégia promissora no tratamento de câncer (SHOJAEI, 2012). Os ensaios de angiogênese (in vitro) para o rastreio desses fármacos tem sido focados em testes de adesão, migração, proliferação e tubulogênese por células endoteliais em resposta a agentes inibidores ou estimuladores exógenos (JAIN, 2012). A observação de que células tumorais também podem formar redes tubulares e expressar fenótipo endotelial, sugeriu que inibidores da angiogênese poderiam inibir a formação de mimetismo vasculogênico em células tumorais. No entanto, o tratamento com inibidores da angiogênese não se mostrou eficaz para inibir o mimetismo vasculogênico em células de melanoma (VAN DER SCHAFT *et al*., 2004), sugerindo que essas células tumorais plásticas não adquirem sensibilidade aos mesmos fármacos utilizados na angiogênese.

Durante muitos anos os modelos 2D têm sido utilizados como modelos pré-clínicos para o rastreio de fármacos com o objetivo de simular o microambiente in vivo. Entretanto, os fármacos não funcionam de forma eficaz in vivo como funcionam em plataformas 2D (BISSELL; RADISKY, 2001). Para superar as limitações presentes na estrutura 2D, um número crescente de estudos, estão sendo realizados em modelos 3D. Plataformas 3D mimetizam o microambiente in vivo devido a sua estrutura e assim induzem interações célula-célula e célula-matriz. Características das células tumorais in vivo, tais como aumento da liberação de fatores de crescimento vascular, aumento da invasividade e potencial metastático, proliferação mais lenta, aumento da resistência a fármacos anticancerígenos são também comportamentos presentes em modelos 3D (BOND, 2005; LIANG *et al*., 2011; TAN; MARRA, 2010).

Muitas MEC comerciais, como Matrigel® e Geltrex® têm sido utilizadas como suportes 3D de células tumorais. Nessas matrizes de origem animal (sarcoma de rato) os principais componentes são laminina, colágeno IV, entactina, e proteoglicanos de sulfato de heparano e a composição de cada componente pode variar de lote para lote (HUGHES; POSTOVIT; LAJOIE, 2010; KLEINMAN; MARTIN, 2005). Apesar dessas matrizes fornecerem pistas químicas e mecânicas essenciais para o comportamento celular, os resultados são frequentemente inconsistentes devido à variabilidade de lote para lote, composição química indefinida e manuseamento difícil do hidrogel (HUGHES; POSTOVIT; LAJOIE, 2010; KLEINMAN; MARTIN, 2005). O desenvolvimento de novos sistemas de cultura 3D que simulam o microambiente extracelular do tumor pode ser apropriado para testar o comportamento de células de câncer e a sensibilidade das células tumorais e células endoteliais aos fármacos anticancerígenos.

2.3 HIDROGÉIS

Uma plataforma ideal deve proporcionar um ambiente adequado para a adesão, proliferação, diferenciação, migração e invasão celular (PEPPAS *et al*., 2006). Alternativamente, hidrogéis sintéticos têm sido utilizados como plataformas para permitir o crescimento de células tumorais e angiogênese de tumor, através da utilização de moléculas sinalizadoras na matriz. Os hidrogéis fornecem microambientes dinâmicos que se assemelham a MEC, para regular o destino da células através de interações célula-célula ou célula-matriz(EL-SHERBINY; YACOUB, 2013a; MILLER et al., 2010).

A MEC nativa é uma matriz fibrosa altamente complexa composta de proteínas (por exemplo colágeno, laminina, fibronectina, elastina), glicosaminoglicanos (por exemplo, ácido hialurónico, heparina), proteoglicanos (por exemplo, perlecano, sindecano), e fatores de crescimento e desempenha um papel crítico nos comportamentos celulares cruciais como diferenciação, proliferação, invasão e apoptose (KULAR; BASU; SHARMA, 2014). A MEC atua não só como uma estrutura de suporte mecânico para as células, mas também como um ambiente dinâmico bioativo e medeia as funções celulares (RHODES;

SIMONS, 2007). Assim a incorporação de moléculas bioativas em hidrogéis é uma importante estratégia para a fabricação de plataformas que mimetizem o ambiente in vivo (ZHU; MARCHANT, 2011).

2.3.1 Nanocelulose bacteriana (BNC)

A BNC é um hidrogel secretado por bactérias do gênero *Gluconacetobacter* como nanofibras hidrofílicos que se assemelha MEC nativa (RAMBO *et al*., 2008). BNC é composto por monômeros de glicose ligados por ligações β(1–4) glicosídicas de fórmula química $(C_6H_{10}O_5)_n$, (PARK; PARK; JUNG, 2003). A estrutura do hidrogel de BNC lhe confere propriedades únicas, como a capacidade de retenção de água, resistência mecânica, a porosidade e a biocompatibilidade (KLEMM *et al*., 2011).

O hidrogel de BNC formado em cultura estática é caracterizado por uma estrutura de rede fibrosa ultrafina 3D, contendo cerca de 99% de água (KLEMM *et al*., 2001). Quando BNC é produzido em condições estáticas, duas superfícies distintas são formadas. O lado que compreende a interface ar / líquido tem uma densidade mais elevada de fibra (superfície superior) e do lado oposto mostra uma menor densidade de fibras e uma superfície mais porosa (superfície inferior) (BERTI et al., 2013). Devido as propriedade deste material BNC extensivamente utilizado em aplicações da engenharia de tecidos (COLLA; PORTO, 2014; CZAJA *et al*., 2007; KLEMM *et al*., 2001; RECOUVREUX *et al*., 2011; ZHIJIANG; GUANG, 2011).

Algumas tentativas têm sido realizadas para combinar BNC com moléculas bioativas (BROWN; LABORIE; ZHANG, 2012; PERTILE *et al*., 2012) no entanto, a formação destes materiais dependem de ligações físicas (adsorção, revestimento, etc.). A imobilização eficaz de moléculas bioativas na estrutura BNC representa uma oportunidade interessante para explorar a sinalização molecular de BNC em células animais.

Muitos autores descreveram hidrogéis de BNC como plataforma para liberação de fármacos (BODHIBUKKANA *et al*., 2006; SUEDEE *et al*., 2008; TROVATTI *et al*., 2012). No entanto, a

investigação do uso de BNC como um modelo tumoral tem sido muito limitada.

Neste trabalho, imobilizamos duas diferentes moléculas bioativas na superfície de hidrogéis BNC, heparina e um peptídeo derivado de laminina, IKVAV. A heparina, um glicosaminoglicano que contém cargas aniônicas, tem sido utilizada devido a sua ampla afinidade com várias moléculas de sinalização. O uso da heparina no desenvolvimento de suportes para a engenharia de tecidos tem mostrado que os glicosaminoglicanos melhora significativamente a angiogênese (CAPILA; LINHARDT, 2002; RAJANGAM *et al*., 2006). O peptídeo IKVAV, derivado de laminina, tem sido relatado como um potente estimulador do crescimento do tumor, metástase, protease de ativação/secreção e angiogênese (ASSAL; MIE; KOBATAKE, 2013; HOSSEINKHANI *et al*., 2013). Além disso, o peptídeo IKVAV foi reportado como migração de células endoteliais e formação de rede tubular que ocorre através da interação com o receptor desconhecido na superfície de células de tumor (GRANT *et al*., 1992; KIBBEY *et al*., 1994).

3 IMMOBILIZATION OF HEPARIN ON BACTERIAL NANOCELLULOSE HYDROGELS INDUCES HUMAN ENDOTHELIAL CELL TUBULOGENESIS

The work presented in this chapter was supported by the Brazilian National Council for Scientific and Technological Development (CNPq) and CAPES. The microscope images were obtained at the Central Laboratory of Electron Microscopy at the Federal University of Santa Catarina (UFSC). A manuscript with the results contained in this chapter is being prepared for submission.

Abstract

Models that mimic the angiogenesis initial processes, as adhesion, migration, proliferation and tubulogenesis, are extremely valuable for investigating the action of new anti-cancer drugs. There is still a need for an angiogenesis model that reflects in vivo environment, without the use of many factors that can interfere in the results. To address this challenge, we developed a 3D matrix well- defined based on covalently immobilization of heparin (HEP) on bacterial nanocellulose (BNC) hydrogels. First BNC hydrogel was oxidized with HNO_3/H_3PO_4-$NaNO_2$, followed by derivatization with 1-ethyl-3-(3-dimethylaminopropyl)-carbodiimide (EDC), and finally heparin was immobilized on the hydrogel by covalent bonds. Successful immobilization of the heparin into BNC hydrogel was confirmed by techniques for material characterization and through toluidine blue test was measured the amount of immobilized haparin. Human umbilical vein endothelial cells (HUVECs) were seeded on bottom and top surfaces of hydrogels and cell behavior was observed. The bottom surface of BNC–HEP is capable of supporting cell adhesion, proliferation and tubulogenesis induction. Results here presented indicate that the tubulogenesis induction can be controlled by interactions with bioactive molecule, heparin, instead of soluble biomolecule or complex materials, which would make the production of materials for study of endothelial cells and drug screening, cheaper and more easily controlled.

Keywords: Bacterial nanocellulose; heparin; human umbilical vein endothelial cells; angiogenesis; tubulogenesis

3.1 INTRODUCTION

Cancer drug development costs approximately $1 billion [1], being that just 10% of new cancer drugs really has been effective, adding some weeks or months to a patient's life, rather than years [1, 2]. The low efficiency of the new cancer drugs has been related to the failure of pre-clinical screening and the inconsistent in vitro models used to predict in vivo drug response [2]. Two-dimensional (2D) in vitro models have been used as pre-clinic models to simulate the in vivo microenvironment [3–7]. However, 2D surfaces do not mimic the complex properties of three-dimensional (3D) microenvironment of tissues in vivo [4, 5]. The 3D extracellular matrices (ECM) have been used to resemble the in vivo environment, mimicking molecular and cellular signals able to regulate cell mechanisms, such as related to the tubulogenesis process, in the tumor angiogenesis [8, 9].

Angiogenesis, new blood vessels formation from the existing vasculature, is essential for tumor growth and metastasis [10]. Initially, tumor cells grow without blood vessels support, however with the increasing on the tumor size, cancer cells require nutrients to keep growing. Those nutrients are supplied by the recruitment of new blood vessels (bringing oxygen and other essential cell components) until the tumor site. The blood vessels recruitment arises when tumor cells release endothelial signals, such as angiogenic factors and cytokines. Those recruited blood vessels will be responsible to spread tumor cells in other tissues and organs by a mechanism knowing as metastasis [10, 12]. Briefly, in the early recruitment of blood vessels, angiogenesis has been an attractive target for the development of novel anti-cancer drugs that could be able to block the migration of endothelial cell to cancer site avoiding the proliferation of tumor cells [13].

Angiogenesis assays (in vitro) have been used for the screening of anti-cancer drugs in some stages of angiogenesis, such as: endothelial cells adhesion, migration, proliferation and tube formation [14, 15]. Actually, tubulogenesis assay have been performed on 3D commercial

matrixes, as Matrigel® (Corning), Cultrex® (Sigma Aldrich) and Geltrex® (Thermo Fisher Scientific), that reproduce tumor environment [16, 17]. However, the use of those commercial matrixes for cancer drugs screening produce inconclusive results due to their chemical variability from bacth-to-bacth which difficult the standartization of pre-clinical tests [18]. Consequently, there is an urgent demand regarding to the development of 3D model platforms with a well-established chemical (minimal complexity) and microstructural properties that mimics the tumor ECM. Those 3D platforms could provide essential characteristics to direct and control the behavior related to several stages of cancer progression, as tumor tubulogenesis and tumor angiogenesis.

Hydrogels have been widely used in tissue engineering and medicine regenerative applications, because their mechanical and structural properties could mimic the ECM of many human tissues [19]. Hydrogels surface modifications by the immobilization of bioactive molecules seems to be a strategy to control and guide interactions between cells and hydrogel surfaces [20, 21]. Bacterial nanocellulose hydrogels (BNC) have been synthesized during fermentation of bacteria from *Gluconacetobacter* genus [22]. On static fermentation the bacteria secrete BNC hydrogels containing two distinct surfaces [23]. BNC surface synthesized in the air/liquid interface has been characterized by a high density of fibers (named top surface) and the another surface presents higher porosity (named bottom surface) [24]. BNC hydrogels resemble ECM concerning important properties related to the 3D nanofibrous microstructure [24, 25]. From their interesting microstructure, BNC have been a promisor material for biomedical applications [26, 29].

Structural ECM proteins (elastin, laminin, collagen and fibronection), growth factors (vascular endothelial growth factor (VEGF) and basic fibroblast growth factor (bFGF)), and glycosaminoglycans (GAGs) as heparin, hyaluronan and chondroitin sulfate have been associated as the components responsible for the induction of neovascularization by the recruitment of endothelial cells [30]. Heparin (HEP), a GAG component, holds anionic charges which have been related with a wide variety of signaling molecules that direct endothelial cell fate [31]. The use of heparin on the development of

tissue engineering scaffolds has shown that GAGs enhance significantly angiogenesis independent of the addition of other exogenous growth factors [32].

In this study, we propose to perform the chemical immobilization of heparin (HEP) on bacterial nanocelulose hydrogels (BNC) as an alternative to induce endothelial cells adhesion, proliferation which could provide an ideal microenvironment to endothelial cells organize themselves as tubulogenic networks on BNC–HEP hydrogels. We pretend also explore the influence of BNC–HEP hydrogels microstructure on endothelial cells behavior seeking for the development of a helpful platform to be used in the screening of anticancer drugs.

3.2 EXPERIMENTAL

3.2.1 Materials

Reagents and chemicals were purchased from Sigma-Aldrich do Brasil Ltd. (São Paulo, SP). Culture media and supplements were purchased from Thermo Fisher Scientific do Brasil Ltd. (São Paulo, SP). Heparin (HEPAMAX-S® sodium heparin - 5000 IU/mL) was supplied by Blau Farmacêutica S.A. (Cotia, SP).

3.2.2 BNC–HEP hydrogels synthesis

3.2.2.1 Preparation of BNC hydrogels

Gluconacetobacter hansenii (strain ATCC 23769) was used to produce BNC hydrogels. *G. hansenii* was cultured in a sterile medium composed of mannitol (25 g), yeast extract (5.0 g), and bactopeptone (3.0 g), diluted in 1 L of water and pH adjusted to 6.5. One hundred microliters of inoculum were locked into mannitol agar to form isolated colonies of bacteria, at 26 °C for 5 days. Thirty single colonies were inoculated into 6 mL of mannitol medium. Subsequently, 5 mL of inoculum were transferred to 45 mL of mannitol medium. Mixture was stirred and transferred to 24 wells plates (1 mL/well). After four days, on static culture conditions at 26 °C, hydrogels formed were removed

and purified in 0.1 M NaOH solution at 50°C for 24 h and then rinsed with distilled water to pH 6.5. Finally, the hydrogels were sterilized by autoclaving (121 °C for 20 min) and kept refrigerated until used.

3.2.2.2 Functionalization of BNC hydrogels with heparin

Heparin was chemically immobilized on BNC hydrogels through an oxidation reaction with HNO_3/H_3PO_4-$NaNO_2$ [33] followed by derivatization with EDC [34]. Thirty milliliter of HNO_3 (68% v/v) were mixed with 15 mL of H_3PO_4 (85% v/v) and 50 BNC were submersed in the solution. Subsequently, 0.63 g of $NaNO_2$ was added and the mixture was stirred at the absence of light at room temperature for 24 h. BNC hydrogels were transferred into 0.2 % (w/w) of glycerol solution during 15 min to remove the residual oxidant. Finally, the samples were washed with acetone and air-dried for 30 min at 60 °C. Oxidized BNC (BNC-OX) were immersed in 45 mL of 0.1 M citrate buffer solution (pH 4.8) containing 2mM of EDC (1-ethyl-3-(3-dimethylaminopropyl) carbodiimide). Those hydrogels were shaking during 24 h at 4°C and after washed with deionized water. Samples were placed in citrate buffer (pH 4.8) containing 1000 IU heparin (v/v) for 24 h at 4 °C with shaking. Finally, BNC–HEP hydrogels were washed with alkaline phosphate buffered saline (PBS) and rinsed with distilled water. Hydrogels were lyophilized at -50 °C for 24 h to perform the chemical and microstructural characterization and they were sterilized by UV before to perform biological in vitro tests.

3.2.3 Characterization of BNC–HEP hydrogels

3.2.3.1 Chemical characterization of BNC–HEP hydrogels

The functional groups on BNC and BNC–HEP were analyzed by Fourier Transformed Infrared Spectroscopy (FTIR). Infrared spectra were recorded on an Agilent spectrophotometer (model Carry 600), with a resolution of 4 cm^{-1}, in a range of 4000-600 cm^{-1}, and using attenuated total reflectance.

3.2.3.2 Determination of heparin content in BNC hydrogels

Toluidine blue colorimetric assay was used to determine the amount of heparin immobilized on BNC–HEP [35]. BNC–HEP hydrogels were immersed in a solution containing 600 µL of toluidine blue and 300 µL of sodium chloride for 1 h at 37 ℃. Afterwards, BNC–HEP were removed from the container and 600 µL of hexane were added. The absorbance of the supernatant solution was measured at 631 nm. The amount of heparin immobilized on BNC–HEP hydrogels was quantitated in comparison with the calibration curve.

3.2.3.3 Characterization of the surface area, pore volume and diameter pore distribution of BNC and BNC–HEP hydrogels

The N_2 adsorption-desorption measurements were carried out at 77 K with a liquid nitrogen trap according to the principle of static volumetric method for BNC and BNC–HEP hydrogels by a Quantachrome NovaWin version 10.01. Surface area (SA) was calculated using Brunauer-Emmett and Teller (BET) equation and pore volume (PV) and pore diameter distribution (PD) were performed by Barrett–Joyner–Halenda (BJH) equation.

3.2.3.4 Microstructural characterization of BNC–HEP hydrogels

Scanning electron microscope (SEM) was performed to analyze the microstructure of top and bottom surfaces of BNC and BNC–HEP, using a JEOL JSM-6390LV microscope at 10 kV. For SEM analysis the hydrogels were frozen and lyophilized for 24 h.

3.2.4 In vitro assays

3.2.4.1 Cytotoxicity

The cytotoxic potential of BNC–HEP hydrogels were evaluated following the direct contact assay, according to ISO 10993-5: 2009 [36]. BNC hydrogels, non cytotoxic material [37], were used as control

group. Immortalized murine fibroblast cells (L929) were cultured in DMEM (Dulbecco's Modified Eagle's Medium) supplemented with 10% of FBS and 1% penicillin/streptomycin. L929 cells were seeded in each well of 24 wells culture plate at 9.0×10^3 cells/cm^2 for 24 h in a humidified atmosphere (5% CO_2 in air) at 37 °C. After that, BNC and BNC–HEP hydrogels were added into each well. After 1, 3 and 7 days of in vitro culture, the metabolic activity of L929 cells were determined by MTS [3-(4,5-dimethylthiazol-2-yl)-5-(3carboxymethoxyphenyl)-2-(4-sufophenyl)-2H-tetrazolium] colorimetric assay from Promega Biotecnologia do Brasil, Ltda. (São Paulo, SP), performed according to the manufacturer's instructions. The plates were kept in a humidified atmosphere (5% CO_2), incubated at 37 °C during 2 h protected from light. Absorbance of supernatants solutions were measured at 490 nm using Micro ELISA reader.

3.2.4.2 HUVECs adhesion on BNC and BNC–HEP hydrogels

Immortalized human umbilical vein endothelial cells (HUVECs) were maintained in RPMI-1640 medium supplemented with 10% FBS, 1% penicillin/streptomycin. HUVECs were seeded at a density of 5.2×10^4 cells/cm^2 on the top and bottom surfaces of BNC and BNC–HEP. HUVEC cells were allowed to attach during 4 h on the hydrogels surface kept on a humidified atmosphere containing 5% of CO_2 at 37 °C. After 4 h, MTS solution was used to quantify the number of metabolically active cells adhered on the hydrogels surface. Qualitative assays were also performed and the adherent cells were fixed with 4% formaldehyde for 30 min and permeabilized with 0.1% Triton X-100 for 5 min at room temperature. To visualize F-actin, cells were stained with Alexa Fluor 546 conjugated to phalloidin and cell nuclei were stained with 4',6-diamidino-2-phenylindole dihydrochloride (DAPI). The HUVECs morphology on the early stage of contact between cells-hydrogels was analyzed by confocal laser scanning microscopy (CLSM, Leica DMI6000 B, Leica Microsystems, Mannheim, Germany).

3.2.4.3 HUVECs Proliferation and morphological behavior on BNC and BNC–HEP hydrogels

Proliferation and behavior were analyzed after 1, 2, 3 and 7 days of in vitro culture of HUVEC cells seeding (5.2×10^4 cells/cm^2) on the both surfaces of BNC and BNC–HEP. After 1, 2, 3 and 7 days, MTS assay was used to quantify the proliferation of metabolically active cells on BNC and BNC–HEP surfaces. The morphological behavior of HUVECs cultured on hydrogels surfaces were also observed by confocal microscopy (Leica DMI6000 B, Leica Microsystems, Mannheim, Germany). For that, HUVECs were fixed and stained with Alexa Fluor 546 conjugated with phalloidin and DAPI. After 7 days of in vitro culture, z-stack images were obtained at 2 x amplification assuming z-spacing of 3 µm per slice and compiled as projections to observe HUVECs distribution over BNC and BNC–HEP surfaces.

3.2.4.4 Tubulogenesis induction

HUVECs were seeded at a density of 105 cells/cm2 on the bottom surface of BNC–HEP hydrogels. Samples were incubated for 24 h in a humidified atmosphere containing 5% of CO2 at 37 °C. After 24 h, samples were fixed with 4% of formaldehyde for 30 min at room temperature. Phase contrast images were taken using an Olympus BX4 microscope (Olympus America Inc.).

3.2.5 Statistical analysis

Data were statistically by one-way analysis of variance (ANOVA) with Tukey test. Values represent the mean ± standard medium error, with $p < 0.05$. All experiments were performed in triplicate at two separated experimental times.

3.3 RESULTS

3.3.1 Functionalization of BNC hydrogels

Figure 1 shown a scheme illustration of the oxidative reaction used to immobilize heparin on BNC hydrogels. BNC were oxidized to convert free hydroxyl groups of BNC in carboxyl groups (Fig. 1a). Those carboxyl groups were activated with EDC allowing the covalent immobilization of heparin (Fig. 1b).

Figure 1. Immobilization reaction of heparin in BNC hydrogels. (a) Oxidation process with HNO3/H3PO4-NaNO2 to convert the free hydroxyl groups of BNC to carboxyl groups, resulting in oxidized BNC (BNC-ox) in the carbon C6. (b) Activation of the carboxyl groups present on the BNC-ox with EDC (coupling agent). Followed by the covalent reaction between active carboxyl groups on BNC-ox and the amine groups of the heparin, resulting in BNC-HEP hydrogel.

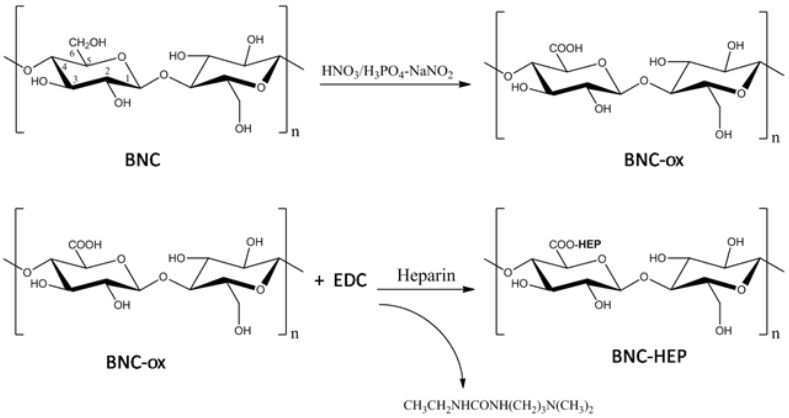

FTIR spectra comproved the presence of heparin on BNC–HEP (Fig. 2). Characteristic bands of BNC appeared at 3345 cm−1 and 2898 cm−1, where the absorption band assigned to hydroxyl groups and hydrogen bonds, respectively [35]. BNC–HEP showed a broad

absorption at 3100–3500 cm-1 which was assigned to N–H stretching absorption and hydrogen bonded hydroxyl groups; other heparin characteristic bands were observed at 1701 cm−1 (C=O) and 1248 cm-1 (S=O) [38–40]. The amount of heparin immobilized on BNC hydrogels was quantified by toluidine blue dye assay which revealed a density of immobilization of 4.7 μg ·cm-2, approximately 1% of BNC dry weight.

Figure 2. FTIR spectroscopy of BNC and BNC-HEP hydrogels. FTIR spectra of BNC with characteristic groups hydroxyl (OH) and alkanes (CH). BNC-HEP heparin immobilized BNC with groups characteristic of heparin as carbonyl (C=O), sulfonic (S=O) and hydroxyl (OH).

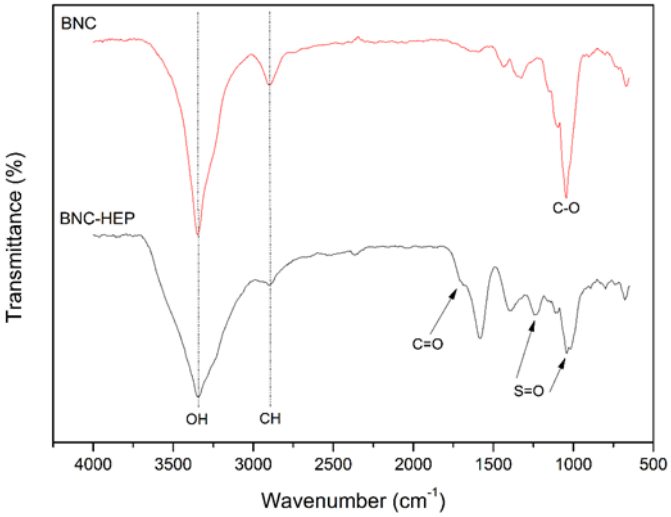

The average of pore diameters distribution (PD), surface area (SA), pore volume (PV) were quantified by nitrogen structure adsorption–desorption. BNC and BNC–HEP showed a similar PD average, ranging from 3.5-30.3 nm to BNC and 3.5-30.8 nm to BNC–HEP. The values obtained to SA and PV were shown in Table 1. In comparison to the BNC, SA and PV of BNC–HEP decreased

approximately 14% and 11%, respectively, after heparin immobilization.

Table 9. Surface area (SA) and pore volume (PV) of BNC and BNC-HEP hydrogels.

Sample	SA (m^2/g)	PV (cm^3/g)
BNC	132.812	0.215
BNC-HEP	114.144	0.190

SEM micrographs related to the top and bottom surfaces of BNC and BNC–HEP hydrogels were shown in Figure 3. BNC hydrogels were characterized by an entangle arrangement of BNC fibers on top surface and with a porous arrangement of fibers on the bottom surface according with described in the literature (Fig. 3a). The top surface of BNC–HEP (Fig. 3d) kept the same microstructure observed on the top surface of BNC (Fig. 3b). Moreover, the bottom surface of BNC–HEP showed a similar microstructure observed on the bottom surface of BNC (Fig. 3a).

Figure 3. SEM micrographs of freeze-dried BNC and BNC-HEP samples. (a) bottom surface BNC, (b) top surface BNC, (c) bottom surface BNC-HEP and (d) top surface BNC-HEP.

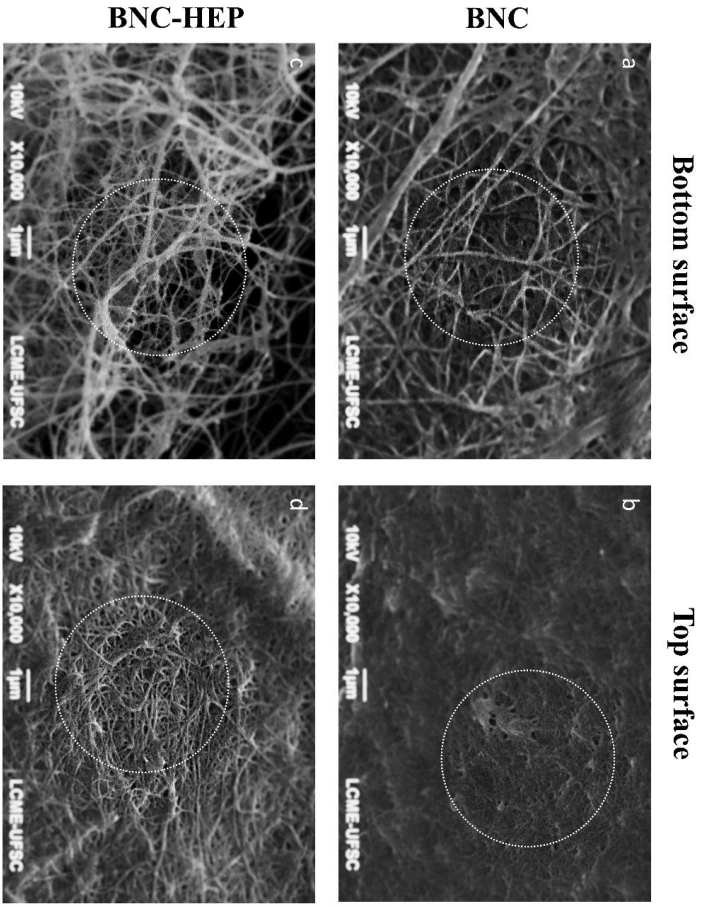

3.3.2 Cytotoxicity

Direct contact between L929 cells and BNC–HEP hydrogels showed that those materials did not induce any cytotoxic effect on L929 cells during 7 days of in vitro culture. The metabolic activity of L929 cells cultured on contact direct with BNC–HEP hydrogels were 96% (1 day), 111% (3 days) and 108% (7 days) compared to BNC hydrogels (100%) (Fig. 4). Significant differences were not observed when compared the metabolic activity of L929 cells cultured on contact direct with BNC and BNC–HEP hydrogels.

Figure 4. Metabolic activity of L929 cells after direct contact with BNC and BNC-HEP hydrogels, during 1, 3 and 7 days. BNC hydrogels was used as reference (100%).

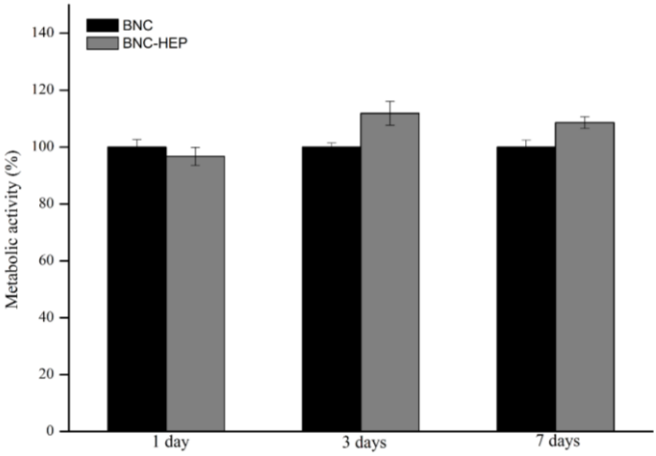

3.3.3 HUVECs adhesion on BNC and BNC–HEP hydrogels

HUVECs were seeded on the top and bottom surfaces of BNC and BNC–HEP to quantify the number of metabolically active cells

adhered on the hydrogels surfaces. After 4 h of seeding, there were 232% more HUVECs adhered on the top surface of BNC–HEP than on the same surface of BNC. On the bottom surfaces, the adhesion of HUVECs was 71% higher on BNC–HEP than on the same surface of BNC (Fig. 5).

Figure 5. Percent adherent HUVECs metabolically active on both surfaces on BNC-HEP hydrogels during 4 h. BNC hydrogels was used as reference (100%). * significantly diferente, $p<0.05$.

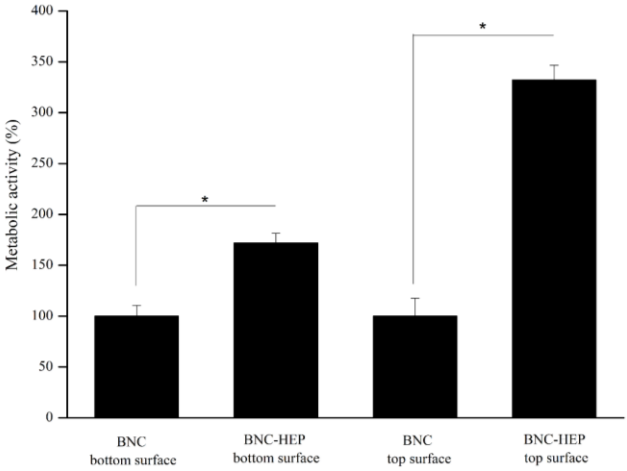

The morphology of HUVECs cultured on BNC and BNC–HEP was evaluated by CLSM images in the early contact (4 h) between cells and hydrogels (Fig. 6). HUVECs were adhered on BNC and BNC–HEP surfaces and they showed a predominantly rounded morphology. Solely, on the bottom surface of BNC and BNC–HEP was possible to observe some spreaded cells (Fig. 6a, b). On the top surface of BNC and BNC–HEP any spreaded cells were observed (Fig. 6d).

Figure 6. CLSM images of HUVECs cultivated after 4 h on the bottom and top surfaces of BNC and BNC-HEP. HUVECs were stained with Alexa Fluor 546 conjugated to phalloidin (red) and DAPI (blue). (a) HUVECs on the bottom surface of BNC, (b)HUVECs on the top surface of BNC, (c) HUVECs on the bottom surface of BNC-HEP and (d) HUVEC cells on the top surface of BNC-HEP.

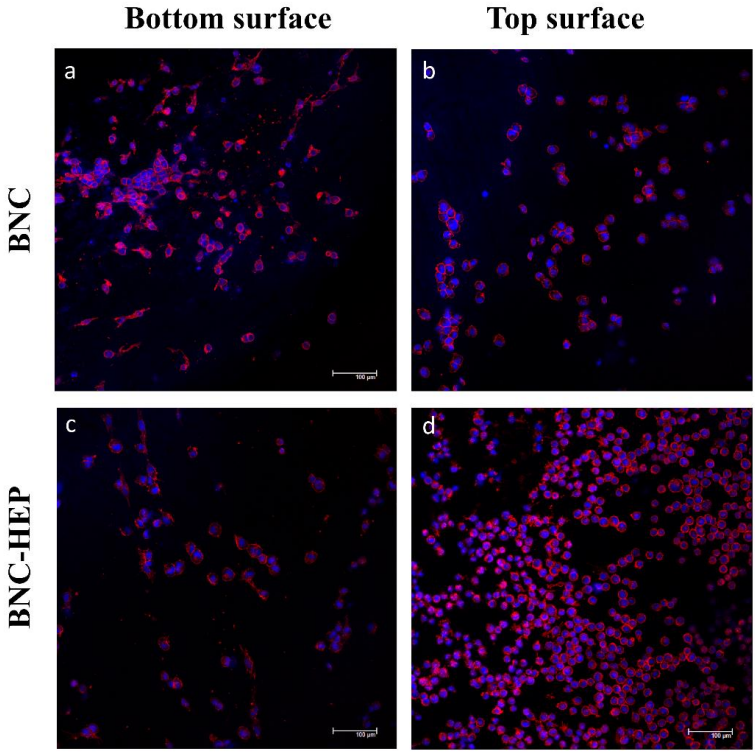

3.3.4 Proliferation and morphology of HUVECs on BNC and BNC–HEP hydrogels

MTS assay was performed after 1, 2, 3 and 7 days of HUVECs cultured on the top and bottom surfaces of BNC and BNC–HEP hydrogels to analyze the influence of chemical surface and

microstructure of those hydrogels on HUVECs proliferation and morphology. An increase on the number of HUVECs metabolically active was observed when cells were cultured on both surfaces of BNC–HEP compared to BNC (Fig. 7). There were significant differences on the number of proliferative HUVECs cultured on the top surface of BNC compared to top surface of BNC–HEP. The proliferation of HUVECs on the top surface of BNC–HEP were 126% (1 day), 75% (2 days), 85% (3 days) and 102% (7 days) higher than on top surface BNC (100%). On the bottom surfaces, HUVECs showed a similar proliferative profile when cultured on BNC and BNC–HEP until three days of culture. Significant differences on bottom surfaces were observed just after 7 days of culture where HUVECs showed an increase on the number of proliferative cells (9%) on the bottom surface of BNC–HEP compared to bottom surface of BNC.

Figure 7. HUVECs metabolic activity on BNC and BNC-HEP during 7 days.

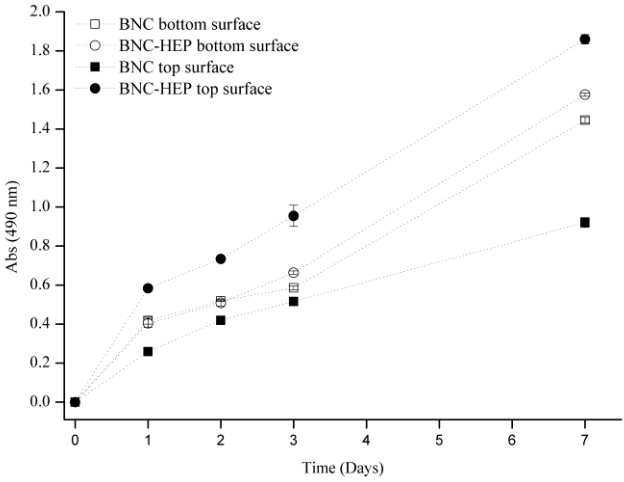

HUVECs morphology was investigated by confocal microscopy during the 7 days of culture on BNC and BNC–HEP. HUVECs cultured during 1 day on the bottom surfaces of BNC and BNC–HEP were

elongated and interconnected (Fig. 8a, d). Moreover, HUVECs began to align on the bottom surface of the BNC–HEP (Fig. 8d) and at the end of two days of culture those cells were completely aligned and arranged as tubulogenic networks (Fig. 8e). On the third day of culture HUVEC cells still proliferative increasing the number of cells and covering the entire on the bottom surface of BNC–HEP (Fig. 8f). Tubulogenic networks formation were not observed on the bottom surface of BNC over 3 days of culture (Fig. 8a-c). HUVECs cultured on the top surface of BNC and BNC–HEP did not organized themselves as tubular networks and those cells adhered with a rounded morphology over the first three days of culture. On the top surface of BNC–HEP was possible to observe a higher number of HUVECs compared to top surface of BNC (Fig. 8j-l). After 1 day of culture, HUVECs formed a monolayer that covered the entire top surface of BNC–HEP (Fig. 8j). On the second and third day of culture, HUVECs formed multilayers on top surface of BNC–HEP hydrogels (Fig. 9k, l). The top surface of BNC showed a lower number of proliferative HUVECs compared to BNC–HEP (Fig. 8g-i).

On seventh day of culture, HUVECs formed multilayers on both surfaces of BNC and BNC–HEP. In Figure 9 is possible to observe the migration and arrangement cell into hydrogels and cell multilayerformation. Due to cell growth in seven days was no longer possible to observe similar structures angiogenesis in the bottom surface of BNC-HEP (Fig. 9e-h). In the bottom surface of BNC hydrogels, HUVEC cells continued elongated although in the multilayer cells (Fig. 9a-d). Top surface of BNC-HEP shows the cells multilayer occupying all hydrogel. In addition, it is possible to observe the presence of elongated cells and well cell aligned on the hydrogel (Fig. 9i-l). Top surface of BNC showed few cells sprawling in the seventh day of culture, and rounded morphology prevailing over the seven days of growth (Fig. 9m-p).

Figure 8. CLSM images of HUVECs cultivated on the bottom and top surfaces of E and BNC-HEP hydrogels during 3 days. HUVECs were stained with Alexa Fluor conjugated to phalloidin (red) and DAPI (blue). (a-c) HUVECs on the bottom surfac BNC over 1, 2, and 3 days, respectively, (d-f) HUVECs on the bottom surface of B HEP over 1, 2 and 3 days, respectively, (g-i) HUVECs on the top surface of BNC 1, 2 and 3 days, respectively and (j-l) HUVECs on the top surface of BNC-HEP ov 2 and 3 days, respectively.

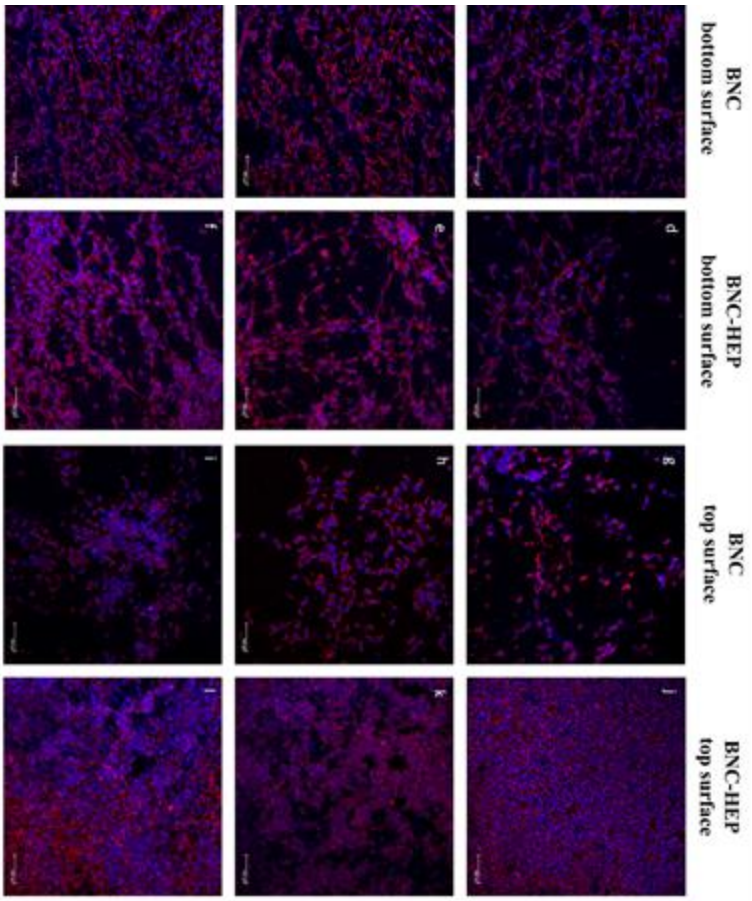

Figure 9. HUVECs interactions into hydrogels on seventh day. The projections were taken at 3 µm per slice. (a-d) HUVECs on the bottom surface of BNC. Depth of images are 30.5, 15.6, and 3.6 µm, respectively. (e-h) HUVECs on the bottom surface of BNC-HEP. Depth of images are 0.9, 11.9, and 19.9 µm, respectively. (i-l) HUVECs on the top surface of BNC. Depth of images are- 39.7, 15.8 and 3.8 µm, respectively. (m-p) HUVECs on the top surface of BNC HEP. Depth of images are 15.4, 5.4, and 20.3 µm, respectively.

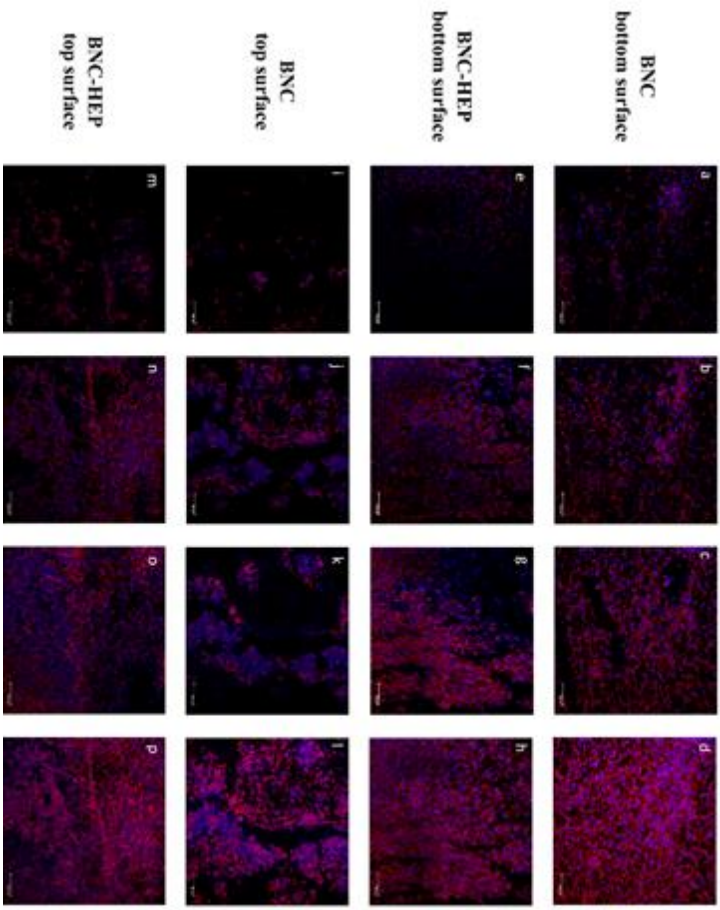

3.3.5 Tubulogenesis induction

HUVECs were able to interconnect and aligne theirselves when cultured on the bottom surface of BNC–HEP. Then, a larger amount of HUVECs (10^5) were sow on the bottom surface of BNC–HEP, to form more tubulogenesis established patterns. After 24 hours of culture, HUVECs were aligned and organized as tubulogenic networks on the bottom surface of BNC–HEP (Fig. 10 and 11). In detail, Figure 10 showed the formation of endothelial tubulogenic networks containing loops and branch points. Figure 11 showed the presence of endothelial tip cells, characterized by cell protrusions called filopodia. Following the endothelial tip cells were observed endothelial stalk cells.

Figure 10. Phase contrast images of tubulogenesis process of HUVECs cultured on the bottom surface of BNC-HEP after 24 h. Red arrows indicate branching points and the loops are represented by red rings. Scale bars represent 100 μm.

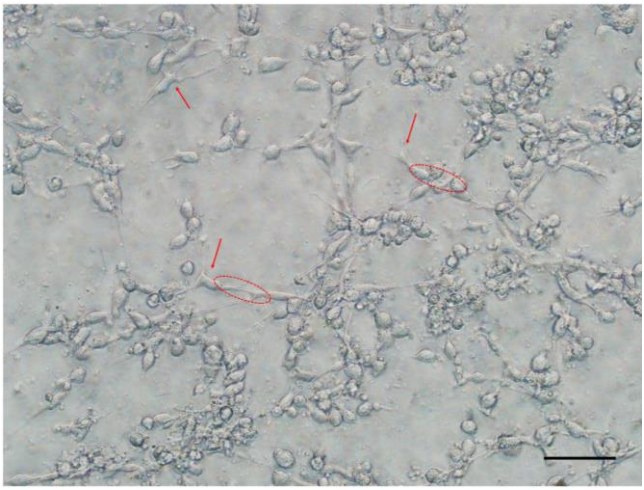

Figure 11. Phase contrast images of tubulogenesis process of HUVECs cultured on the bottom surface of BNC-HEP after 24 h. Red arrows indicate tip cells. Stalk cells are represented by rings. Scale bars represent 100 µm.

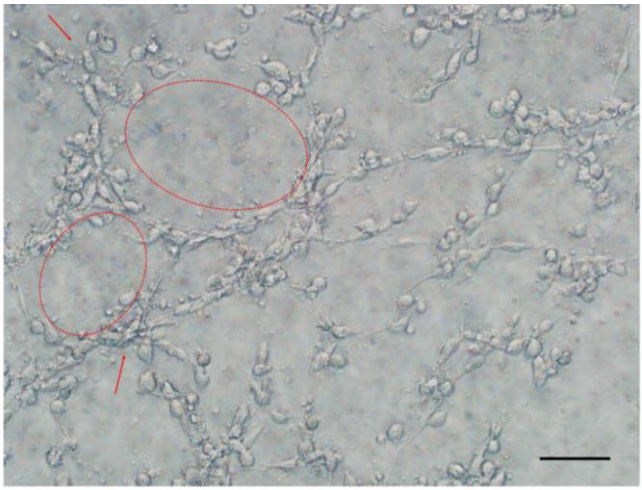

3.4 DISCUSSION

The evaluation of the effectiveness of anti-tumor drugs must be investigated by several phases of pre-clinical trials [42]. One of the main phase of the pre-clinical-trial has been related to the ability of a specific anti-tumor drug inhibit the formation of blood vessels (angiogenesis assays) by the tumor cells. Moreover, pre-clinical trial phases also investigate the endothelial cell behavior analyzing their potential to adhere, migrate, proliferate and form vessel tubes [43]. Actually, in vitro models of pre-clinical-trials have been doing using 2D cell culture plates or commercial ECM extracted from tumor of murine (tubulogenesis assay) which not mimic the in vivo tumor microenvironment. Commercial ECM have been associated with chemical variations from batch to batch [16]. In this context, we propose the development of a novel 3D tubulogenesis platforms with no chemical stability and variation to perform the screening of anti-tumor

drugs to affect the recruitment of vascular blood vessels and also to study the behavior of endothelial cells (adherence, proliferation and migration), subsequently. A novel 3D platforms were successfully developed by the immobilization of heparin (HEP) on BNC hydrogels.

BNC–HEP hydrogels were produced by an oxidative reaction [33] where heparin was covalently bonded on the carboxyl group of BNC. The chemical immobilization of HEP were confirmed by FTIR analysis through the presence of characteristic bands (C = O and S = O). Hydrogels that contain porous surface have been related as an ideal surface for HUVECs culture [44]. Based on distribution of pores diameters BNC and BNC–HEP were classified as mesoporous polymers (sizes between 2 to 50 nm) [41]. Mesoporous hydrogels have been highlighted in tissue engineering applications, since the pores in the nanometer range could support cell adhesion and proliferation [45]. The surfaces areas found on BNC and BNC–HEP were over than 100 m^2/g which were the highest surface area found in the literature (from 12.3 to 22.8 m^2/g) [46, 47]. We believe that the genus of the bacteria used to produce BNC hydrogels and also the fermentation time were important parameters to support those surface area value to BNC.

SEM micrographs revealed microstructural differences between bottom and top surface of BNC agreeing with the observations already published [23, 38, 46, 48]. Yizao Wan and collaborators (2011) adsorbed (immersed on HEP solution) heparin on BNC hydrogels, however they did not observed any microstructural difference between BNC and BNC functionalized with heparin [38]. Those results suggested that the oxidation process used in our work to immobilize chemically HEP may changed the microstructure of BNC–HEP. As result we found that the immobilization of HEP by oxidative reaction became the bottom surface of BNC–HEP more porous than BNC.

Based on our results we found that BNC and BNC–HEP were no cytotoxic hydrogels for tissue engineering applications through ISO 10993-5: 2009 [29]. The cytotoxicity potential of BNC hydrogels was also evaluated by Saska et al., (2012) which demonstrated absence of in vitro cytotoxicity effects caused by BNC [37]. Other authors also tested the cytotoxicity BNC-chitosan hydrogels functionalized with heparin, and those materials were not cytotoxic [38]. Our results also showed

that the immobilization of heparin was not cytotoxic to L929 cells. BNC and BNC–HEP were used to investigate the behavior of HUVECs cultured on both surfaces of those hydrogels. BNC–HEP hydrogels promoted an increasing on cell adhesion when compared to BNC. Bottom surface of BNC–HEP showed 70% more HUVECs adhered compared to the same surface of BNC. When HUVECs were cultured on the top surface of BNC–HEP they adhered twice more compared to the top surface of BNC. In addition, there were no significant differences between the number of adhered cells on the top and bottom surfaces of BNC ($p < 0.05$). Top and bottom surfaces of BNC–HEP were able to support and increase the number of HUVECs adhered. However, after 4 h of seeding, the bottom surfaces of both hydrogels were able to induce the spreading of HUVECs. The increasing on the number of adhered HUVECs must be related to heparin immobilization on BNC hydrogels. When HUVECs were cultured with heparin as a component of culture medium, they also showed an increasing on the expression of gene related to cell adhesion [49].

An increasing on HUVECs proliferation was observed when these cells were cultured on the both surfaces of BNC–HEP. The number of proliferative HUVECs on the bottom surfaces of BNC and BNC–HEP were significantly different only after 7 days of culture. HUVECs behavior were completely dependent of the surface of seeding. HUVECs cultured on the top surfaces of BNC and BNC–HEP were morphologically rounded. Unlike, HUVECs cultured on the bottom surfaces of BNC and BNC–HEP were elongated and they maintained cell-cell interactions. We noted that HUVECs cultured on the bottom surface of BNC–HEP were able to contact themselves and they were aligned in network-like.

Tubulogenesis assays have been usually carried out by seeding endothelial cells on a commercial ECM (ECM from animal origin, such as Matrigel® or Geltrex®) [16, 50]. Cell behavior as tubes, branch points and loops have been used to quantify tubulogenesis process [50]. When 10^5 cells/cm^2 HUVECs were seeded on the bottom surface of BNC–HEP, these cells auto-organize themselves as vascular networks, tubulogenesis.

After 24 h, HUVECs cultured on the bottom surface of BNC–HEP formed a well-organized vascular network containing several capillar sprouts. Capillary sprouts have been composed by the presence of endothelial tip and stalk cells. Endothelial tip cells coordinate cells alignment through the filapodios that produce attractive and repulsive directional signals being the most important phenotype to direct branch points, interconnectivity and functionability to the vascular network The endothelial tip cells were followed by aligned proliferative cells, denominated stalk cells [51, 52]. Endothelial stalk cells established adherent points and tight junctions to ensure the endothelial stability required to form the nascent vascular lumen [53]. The presence of endothelial stalk cells indicate high cell proliferation on BNC–HEP. Endothelial branch points and loops have been essential on tubulogenesis process. The analysis of the number of branch points and loops of in vitro assays provided an useful measurement of the outgrowth and extension of pre-angiogenesis network [54].

Commercial ECM contain many pro-angiogenic factors which make it difficult to assess the real influence of drugs on the tubulogenesis process [50]. In addition, tubulogensis formed on those commercial ECM have been reported as quite homogeneous in length and shape which not represent angiogenesis in vivo [55]. The same problem was also observed on artificial matrices where several molecules were used to signalize tubulogenesis to HUVECs [30, 56, 58]. Here, we produced a 3D platform based on BNC–HEP hydrogels that induce tubulogenesis on human endothelial cells. Further investigations will be performed to analyze the influence of known anticancer drugs on the tubulogenesis formed on BNC–HEP hydrogels. Thus, our results showed some evidences that BNC–HEP hydrogels could be used to overcome the problems actually found in the current tubulogenesis platforms.

Finally, our results proved that not only the presence of HEP was important to signalize the HUVECs to form the vessel tube network, but also the microstructure of BNC. Our results reinforce the idea that chemical and physical fields should be considered on the design of novel tissue engineering constructions.

3.5 CONCLUSIONS

The BNC–HEP hydrogels were obtained via covalent bondsbetween heparin and oxidized BNC. The behavior of cultured HUVEC cells on both surfaces (top and bottom) of the BNC and BNC–HEP hydrogels was dependent on the microstructure and chemical composition these materials. Top surface of BNC–HEP was able to increase the adhesion and proliferation of HUVEC cells compared to BNC. Morever, bottom surface of BNC–HEP was able to induce tubulogenesis in HUVEC cells after 24 h culture. Thus, BNC–HEP was able to induce early stages of angiogenesis in HUVECs, with the use of only a bioactive molecule, heparin. The use of this material as a screening anti-angiogenic can overcome the difficulties in obtaining reliable results in this animal platforms currently available. Furthermore, BNC–HEP hydrogels are readily available material, reproducible and inexpensive.

3.6 REFERENCES

[1] D. W. Light and H. Kantarjian, “Market spiral pricing of cancer drugs,” Cancer, vol. 119, no. 22. pp. 3900–3902, 2013.

[2] M. Gevaert, “Engineering 3D Tissue Systems to Better Mimic Human Biology,” in The bridge: Linking Engineering and Society, vol. 42, no. 4, pp. 48–55, 2012.

[3] S. J. Mandriota and M. S. Pepper, “Vascular endothelial growth factor-induced in vitro angiogenesis and plasminogen activator expression are dependent on endogenous basic fibroblast growth factor.” J. Cell Sci., vol. 110, pp. 2293–2302, 1997.

[4] R. Montesano and L. Orci, “Phorbol esters induce angiogenesis in vitro from large-vessel endothelial cells.,” J. Cell. Physiol., vol. 130, no. 2, pp. 284–291, 1987.

[5] C. M. Nelson and M. J. Bissell, “Modeling dynamic reciprocity: Engineering three-dimensional culture models of breast architecture, function, and neoplastic transformation,” Seminars in Cancer Biology, vol. 15, no. 5 SPEC. ISS. pp. 342–352, 2005.

[6] M. S. Pepper, N. Ferrara, L. Orci, and R. Montesano, “Potent synergism between vascular endothelial growth factor and basic fibroblast growth factor in the induction of angiogenesis in vitro,” Biochem. Biophys. Res. Commun., vol. 189, no. 2, pp. 824–831, 1992.

[7] A. A. Ucuzian and H. P. Greisler, “In vitro models of angiogenesis,” in World Journal of Surgery, vol. 31, no. 4, pp. 654–663, 2007.

[8] Z. Chen, A. Htay, W. Dos Santos, G. T. Gillies, H. L. Fillmore, M. M. Sholley, and W. C. Broaddus, “In vitro angiogenesis by human umbilical vein endothelial cells (HUVEC) induced by three-dimensional co-culture with glioblastoma cells,” J. Neurooncol., vol. 92, no. 2, pp. 121–128, 2009.

[9] P. Correa de Sampaio, D. Auslaender, D. Krubasik, A. V. Failla, J. N. Skepper, G. Murphy, and W. R. English, “A heterogeneous in vitro three dimensional model of tumour-stroma interactions regulating sprouting angiogenesis,” PLoS One, vol. 7, no. 2, 2012.

[10] J. Folkman, “Tumor angiogenesis: therapeutic implications.,” N. Engl. J. Med., vol. 285, no. 21, pp. 1182–1186, 1971.

[11] S. M. Weis and D. A. Cheresh, “Tumor angiogenesis: molecular pathways and therapeutic targets,” Nature Medicine, vol. 17, no. 11. pp. 1359–1370, 2011.

[12] G. Bergers and L. E. Benjamin, “Tumorigenesis and the angiogenic switch.,” Nat. Rev. Cancer, vol. 3, no. 6, pp. 401–410, 2003.

[13] R. K. Jain, “Delivery of molecular and cellular medicine to solid tumors,” Advanced Drug Delivery Reviews, vol. 64, no. SUPPL. pp. 353–365, 2012.

[14] A. F. Karamysheva, “Mechanisms of angiogenesis,” Biochem., vol. 73, no. 7, pp. 751–762, Jul. 2008.

[15] T. H. Adair and J.-P. Montani, Angiogenesis, vol. 2, no. 1. 2010.

[16] H. K. Kleinman and G. R. Martin, “Matrigel: Basement membrane matrix with biological activity,” Semin. Cancer Biol., vol. 15, no. 5 SPEC. ISS., pp. 378–386, 2005.

[17] G. Y. Lee, P. A. Kenny, E. H. Lee, and M. J. Bissell, “Three-dimensional culture models of normal and malignant breast epithelial cells.,” Nat. Methods, vol. 4, no. 4, pp. 359–365, 2007.

[18] G. D. Prestwich, “Simplifying the extracellular matrix for 3-D cell culture and tissue engineering: A pragmatic approach,” J. Cell. Biochem., vol. 101, no. 6, pp. 1370–1383, 2007.

[19] I. M. El-Sherbiny and M. H. Yacoub, “Hydrogel scaffolds for tissue engineering: Progress and challenges,” Glob. Cardiol. Sci. Pract., vol. 2013, no. 3, p. 38, Sep. 2013.

[20] R. Murugan and S. Ramakrishna, “Design strategies of tissue engineering scaffolds with controlled fiber orientation.,” Tissue Eng., vol. 13, no. 8, pp. 1845–1866, 2007.

[21] S. P. Massia, J. Stark, and D. S. Letbetter, “Surface-immobilized dextran limits cell adhesion and spreading,” Biomaterials, vol. 21, no. 22, pp. 2253–2261, 2000.

[22] F. Lina, Z. Yue, Z. Jin, and Y. Guang, “Bacterial Cellulose for Skin Repair Materials,” Biomed. Eng. – Front. Challenges, pp. 250–274, 2009.

[23] F. V. Berti, C. R. Rambo, P. F. Dias, and L. M. Porto, “Nanofiber density determines endothelial cell behavior on hydrogel matrix,” Mater. Sci. Eng. C, vol. 33, no. 8, pp. 4684–4691, 2013.

[24] C. R. Rambo, D. O. S. Recouvreux, C. A. Carminatti, A. K. Pitlovanciv, R. V. Antônio, and L. M. Porto, “Template assisted synthesis of porous nanofibrous cellulose membranes for tissue engineering,” Mater. Sci. Eng. C, vol. 28, no. 4, pp. 549–554, 2008.

[25] D. Klemm, F. Kramer, S. Moritz, T. Lindström, M. Ankerfors, D. Gray, and A. Dorris, “Nanocelluloses: A new family of nature-based materials,” Angewandte Chemie - International Edition, vol. 50, no. 24. pp. 5438–5466, 2011.

[26] K. Cesca, M. L. Cacicedo, V. E. Bossio, G. R. Castro, and L. M. Porto, “BaCarbTM: anovel bioinorganic matrix for local drug delivery,” BMC Proc., vol. 8, no. Suppl 4, p. P77, 2014.

[27] G. Colla and L. Porto, “Development of artificial blood vessels through tissue engineering,” BMC Proc., vol. 8, no. Suppl 4, p. P45, 2014.

[28] D. Klemm, D. Schumann, U. Udhardt, and S. Marsch, “Bacterial synthesized cellulose - Artificial blood vessels for microsurgery,” Prog. Polym. Sci., vol. 26, no. 9, pp. 1561–1603, 2001.

[29] W. K. Czaja, D. J. Young, M. Kawecki, and R. M. Brown, “The future prospects of microbial cellulose in biomedical applications,” Biomacromolecules, vol. 8, no. 1. pp. 1–12, 2007.

[30] N. Afratis, C. Gialeli, D. Nikitovic, T. Tsegenidis, E. Karousou, A. D. Theocharis, M. S. Pav??o, G. N. Tzanakakis, and N. K. Karamanos, “Glycosaminoglycans: Key players in cancer cell biology and treatment,” FEBS Journal, vol. 279, no. 7. pp. 1177–1197, 2012.

[31] I. Capila and R. J. Linhardt, “Heparin-protein interactions.,” Angew. Chem. Int. Ed. Engl., vol. 41, no. 3, pp. 391–412, 2002.

[32] K. Rajangam, H. A. Behanna, M. J. Hui, X. Han, J. F. Hulvat, J. W. Lomasney, and S. I. Stupp, “Heparin binding nanostructures to promote growth of blood vessels,” Nano Lett., vol. 6, no. 9, pp. 2086–2090, 2006.

[33] V. Kumar and T. Yang, “HNO3/H3PO4-NANO2 mediated oxidation of cellulose - Preparation and characterization of bioabsorbable oxidized celluloses in high yields and with different levels of oxidation,” Carbohydr. Polym., vol. 48, no. 4, pp. 403–412, 2002.

[34] T. Y. Liu, W. C. Lin, L. Y. Huang, S. Y. Chen, and M. C. Yang, “Hemocompatibility and anaphylatoxin formation of protein-immobilizing polyacrylonitrile hemodialysis membrane,” Biomaterials, vol. 26, no. 12, pp. 1437–1444, 2005.

[35] J. S. Bae, E. J. Seo, and I. K. Kang, “Synthesis and characterization of heparinized polyurethanes using plasma glow discharge,” Biomaterials, vol. 20, no. 6, pp. 529–537, 1999.

[36] International Organization for Standardization, “Biological Evaluation of Medical Devices Part 5: Tests for In Vitro Cytotoxicity,” Iso 10993–5., vol. 5, pp. 1 – 52, 2009.

[37] S. Saska, L. N. Teixeira, P. Tambasco de Oliveira, A. M. Minarelli Gaspar, S. J. Lima Ribeiro, Y. Messaddeq, and R. Marchetto, “Bacterial cellulose-collagen nanocomposite for bone tissue engineering,” J. Mater. Chem., vol. 22, no. 41, p. 22102, 2012.

[38] Y. Wan, C. Gao, M. Han, H. Liang, K. Ren, Y. Wang, and H. Luo, “Preparation and characterization of bacterial cellulose/heparin hybrid nanofiber for potential vascular tissue engineering scaffolds,” Polym. Adv. Technol., vol. 22, no. 12, pp. 2643–2648, 2011.

[39] G. B. Oliveira, L. B. Carvalho, and M. P. C. Silva, “Properties of carbodiimide treated heparin,” Biomaterials, vol. 24, no. 26, pp. 4777–4783, 2003.

[40] Y. Z. Wan, Y. Huang, C. D. Yuan, S. Raman, Y. Zhu, H. J. Jiang, F. He, and C. Gao, “Biomimetic synthesis of hydroxyapatite/bacterial cellulose nanocomposites for biomedical applications,” Mater. Sci. Eng. C, vol. 27, no. 4, pp. 855–864, 2007.

[41] J. Weber and L. Bergström, “Mesoporous hydrogels: Revealing reversible porosity by cryoporometry, X-ray scattering, and gas adsorption,” Langmuir, vol. 26, no. 12, pp. 10158–10164, 2010.

[42] M. Athar, J. H. Back, X. Tang, K. H. Kim, L. Kopelovich, D. R. Bickers, and A. L. Kim, “Resveratrol: A review of preclinical studies for human cancer prevention,” Toxicology and Applied Pharmacology, vol. 224, no. 3. pp. 274–283, 2007.

[43] W. N. Hait, “Anticancer drug development: the grand challenges.,” Nat. Rev. Drug Discov., vol. 9, no. 4, pp. 253–254, 2010.

[44] S. Yang, K. F. Leong, Z. Du, and C. K. Chua, “The design of scaffolds for use in tissue engineering. Part I. Traditional factors.,” Tissue Eng., vol. 7, no. 6, pp. 679–89, 2001.

[45] S. J. Hollister, “Porous scaffold design for tissue engineering.,” Nat. Mater., vol. 4, no. July, pp. 518–524, 2005.

[46] J. Guo and J. M. Catchmark, “Surface area and porosity of acid hydrolyzed cellulose nanowhiskers and cellulose produced by Gluconacetobacter xylinus,” Carbohydr. Polym., vol. 87, no. 2, pp. 1026–1037, 2012.

[47] H. Jia, Y. Jia, J. Wang, Y. Hu, Y. Zhang, and S. Jia, “Potentiality of bacterial cellulose as the scaffold of tissue engineering of cornea,” in Proceedings of the 2009 2nd International Conference on Biomedical Engineering and Informatics, BMEI 2009, 2009.

[48] J. F. Godinho, F. V. Berti, D. M??ller, C. R. Rambo, and L. M. Porto, “Incorporation of Aloe vera extracts into nanocellulose during biosynthesis,” Cellulose, vol. 23, no. 1, pp. 545–555, 2016.

[49] A. Smailbegovic, R. Lever, and C. P. Page, “The e ? ects of heparin on the adhesion of human peripheral blood mononuclear cells to human stimulated umbilical vein endothelial cells,” vol. 1, pp. 827–836, 2001.

[50] M. W. Irvin, A. Zijlstra, J. P. Wikswo, and A. Pozzi, “Techniques and assays for the study of angiogenesis.,” Exp. Biol. Med. (Maywood)., pp. 1476–1488, 2014.

[51] F. De Smet, I. Segura, K. De Bock, P. J. Hohensinner, and P. Carmeliet, “Mechanisms of vessel branching: Filopodia on endothelial tip cells lead the way,” Arteriosclerosis, Thrombosis, and Vascular Biology, vol. 29, no. 5. pp. 639–649, 2009.

[52] J. Wang, Y. Wan, and Y. Huang, “Immobilisation of heparin on bacterial cellulose-chitosan nano-fibres surfaces via the cross-linking technique,” IET Nanobiotechnology, vol. 6, no. 2, p. 52, 2012.

[53] R. Blanco and H. Gerhardt, “VEGF and Notch in tip and stalk cell selection,” Cold Spring Harb. Perspect. Med., vol. 3, no. 1, 2013.

[54] C. A. Staton, M. W. R. Reed, and N. J. Brown, “A critical analysis of current in vitro and in vivo angiogenesis assays,” International Journal of Experimental Pathology, vol. 90, no. 3. pp. 195–221, 2009.

[55] K. Chwalek, M. V Tsurkan, U. Freudenberg, and C. Werner, “Glycosaminoglycan-based hydrogels to modulate heterocellular communication in in vitro angiogenesis models.,” Sci. Rep., vol. 4, p. 4414, 2014.

[56] a. Zieris, K. Chwalek, S. Prokoph, K. R. Levental, P. B. Welzel, U. Freudenberg, and C. Werner, “Dual independent delivery of pro-angiogenic growth factors from starPEG-heparin hydrogels,” J. Control. Release, vol. 156, no. 1, pp. 32–40, 2011.

[57] A. Zieris, S. Prokoph, K. R. Levental, P. B. Welzel, M. Grimmer, U. Freudenberg, and C. Werner, “FGF-2 and VEGF functionalization of starPEG-heparin hydrogels to modulate biomolecular and physical cues of angiogenesis,” Biomaterials, vol. 31, no. 31, pp. 7985–7994, 2010.

[58] S. Prokoph, E. Chavakis, K. R. Levental, A. Zieris, U. Freudenberg, S. Dimmeler, and C. Werner, “Sustained delivery of SDF-1 from heparin-based hydrogels to attract circulating pro-angiogenic cells,” Biomaterials, vol. 33, no. 19, pp. 4792–4800, 2012.

4 A NOVEL BNC–IKVAV PLATFORM FOR VASCULOGENIC MIMICRY AND OTHER PLASTICITIES OF HUMAN MELANOMA CELLS

The work presented in this chapter was supported by the Brazilian National Council for Scientific and Technological Development (CNPq) and CAPES. The microscope images were obtained at the Central Laboratory of Electron Microscopy at the Federal University of Santa Catarina (UFSC). A manuscript with the results contained in this chapter is being prepared for submission.

Abstract

Invasive melanoma cells involved in the metastasis process usually change their cytoskeletal organization to interact with the surrounding extracellular matrix (ECM). In the metastatic migration, tumor cells adopt distinct shapes, which have been related to their plasticity. The development of a 3D microenvironment that mimics the tumor ECM, inducing tumor cells plasticity, has been required to provide a novel screening 3D platform to test anticancer drugs on the distinct stages of tumor plasticity. We propose to combine IKVAV peptide with bacterial nanocellulose (BNC) hydrogels to develop an ideal 3D model that induces human melanoma, SK–MEL–28 cells, plasticity. IKVAV peptides were chemically immobilized on BNC hydrogels. BNC and BNC–IKVAV hydrogels were characterized by different surface microstructures related to top and bottom of those hydrogels. The cytotoxic assay showed that the presence of IKVAV peptides do not interfere on the non cytotoxic potential of BNC hydrogels. Additionally, BNC-IKAV hydrogels improved the adhesion and proliferation of SK–MEL–28 cells on their top and bottom surfaces. While BNC hydrogels induced SK–MEL–28 cells to organize themselves as tumoroids, BNC–IKVAV hydrogels induced the mesenchymal and amoeboid movements of SK–MEL–28 cells. On the bottom surface of BNC-IKAV hydrogels SK–MEL–28 cells formed well-established networks related to vasculogenic mimicry. Finally, our results showed that BNC and BNC–IKVAV hydrogels could be used as 3D platforms that allow the screening of the effect of antitumor drugs on the different mechanisms of metastasis.

Keywords: Bacterial nanocellulose; IKVAV; human melanoma cells; tumor cells plasticity; vasculogenic mimicry.

4.1 INTRODUCTION

Melanoma is an aggressive form of skin cancer derived from pigment-producing cells called melanocytes. Although melanoma accounts for only 1% of all skin cancers, it is responsible for approximately 80% of all skin cancer-related death [1]. According to the World Health Organization [2], about 132,000 new cases of melanoma are diagnosed worldwide each year. One of the most important parameter that affects the prognosis of melanoma patients is metastasis [3]. Tumor metastasis involved a multistep process which allow tumor cells dissemination from their primary site to form secondary tumors into others tissues and organs. The first stage of tumor metastasis has been denominated as tumor cells invasion [4]. Invasive melanoma cells usually changes their cytoskeletal morphology to become motile and able to degrade the surrounding extracellular matrix (ECM) to initiate the tumor invasion stage [5]. Melanoma cells are highly plastic and they change their pathway of invasion according to the three–dimensional (3D) microenvironment that surrounding them. The surrounding ECMs regulate the metastatic cascade of tumor cells [6].

There are two main pathways of cancer cells invasion that have been described: single tumor cell migration or collective tumor cells migration, which determines how the tumor cells through extracellular matrix barriers [7]. Single tumor cell can be using mesenchymal movements, which are characterized by the elongation of the cytoskeletal, or/and amoeboid movements that are characterized by a rounded shape [8]. Tumor cells when in mesenchymal movements penetrate the surrounding-ECM using subcellular structures called invadopodia that degrades the EMC by cell–matrix contact points [9]. When in amoeboid movements tumor cells externalize cell protrusions that regulates cytoskeleton. Those tumor cell protrusions has denominated as blebs and they usually are positioned on plasmatic membrane of tumor cells [9, 10]. Collective tumor cells invasion has been characterized by the migration of an entire group of tumor cells [7] that organize themselves as clusters, branches, as narrow linear strands

or sheets in an integrated movement that are associate with mesenchymal and/or amoeboid movements [11].

In other kind of tumor plasticity, aggressive melanoma cells organize themselves as vascular channels through a mechanism independent of the tumor angiogenesis, a phenomenon denominated vasculogenic mimicry that refers to the plasticity of aggressive tumor cells to form vascular networks [12]. To construct a vascular mimicry network, tumor cells acquire particular characteristics normally restricted to endothelial cells concerning a well-defined vascular-like structures responsible to conduct blood to supply the tissue oxygen demand and also to allow the invasive process (metastasis) [12–14]. Invasive mechanisms of tumor cells by vascular mimicry development are still not completely understood which compromise the discovering of novel effective drugs to prevent cancer progression and invasiveness [15, 16].

Actually, anticancer drug effectiveness has been examined using two–dimensional (2D) culture plates which not reproduce accurately the in vivo tumor microenvironment [17]. 3D culture platforms have been used to overcome the limitations of 2D culture, owing to their great potential of mimicking the tissue microenvironment in vitro [18, 19]. The most used 3D platforms to study tumor behavior in the concerning of metastasis, plasticity and tubulogenesis and vasculogenic mimicry are natural ECM, such as Matrigel® [20, 21] or Geltrex® [22]. These natural ECM are examples of commercial purified EMC extracted from tumor murine, where major components are laminin, collagen IV, entactin, heparin sulfate proteoglycans and others unknown components. Generally, commercial ECMs often generate inconsistent data which is related to their chemical variability and instability recurrent from batch to batch [22, 23].

Hydrogels have been used as scaffolds for 3D in vitro tests because their structures hold high water content associated with particular mechanical properties that resemble those of natural tissues [24]. Furthermore, hydrogels can be used to deliver soluble or immobilized signaling molecules to cells, acting as a support structure for cell growth and functionalization [25]. Bacterial nanocellulose (BNC) is a hydrogel secreted by Gluconacetobacter hansenii bacteria

with hydrophilic nanofibers that resemble native ECM [29]. The 3D porous structure of BNC gives it unique properties such as water retention capacity, mechanical strength and biocompatibility [26]. It has been established that the cell–biomaterial response influences the microarchitecture of the scaffold surfaces, such as porosity, fiber network structure, surface topology and fiber density [27–29]. When BNC hydrogels were produced under static conditions, two distinct surfaces are formed [30, 31]. The surface that comprises the air/liquid interface has a higher fiber density (top surface) and the opposite surface revealed lower fiber density (bottom surface) [31,32].

Absorption or immobilization of bioactive peptides such as, collagen, fibronectin and laminin, have been used as an approach to increase cell adhesion on hydrogels surfaces [33]. Laminin have been associated with tumor vasculogenic mimicry formation and their absence reduces the expression of genes associated with the plasticity of melanoma cells [34]. Furthermore, peptides, such as laminin plays an important role in cell adhesion, migration, proliferation, neurite outgrowth, and angiogenesis [35]. IKVAV (isoleucine, lysine, valine, alanine, valine) laminin-α1 chain peptide has been related as a potent stimulator of tumor growth, metastasis, protease activation/secretion and angiogenesis [36–39]. Additionally, IKVAV peptide has been reported as endothelial cell migration and tubular network formation which happens through the interaction with unknown receptor at tumor cell surface [40–42].

To date, many studies have been focused on the use of BNC hydrogels as a delivering drug platform for many kinds of cancer treatments [43–45]. However, the best of to our knowledge, there were no studies addressed to the use of BNC hydrogel to understand the behavior of melanoma cells on a 3D microenvironment. Here, we propose the immobilization of IKVAV peptide on BNC hydrogels to explore the influence of the microstructure and the chemical surface properties on the behavior of human melanoma cells (SK–MEL–28). The relationship between the distinct microenvironments, top and bottom surface, of BNC–IKVAV hydrogels may be fundamental to induce particular tumor cells behavior related to tumor metastasis stages, such as vasculogenic mimicry and invasive cell morphology.

4.2 EXPERIMENTAL

4.2.1 Materials

Reagents and chemicals were purchased from Sigma-Aldrich do Brasil Ltda. (São Paulo, SP) and Thermo Fisher Scientific do Brasil Ltda. (São Paulo, SP), unless otherwise stated. Water was distilled and deionized using an EASYpure II water purification system, series 1305, at 18 MΩ of resistance (Thermo Fisher Scientific). IKVAV (Ile-Lys-Val-Ala-Val) peptide was synthetized by Genome Biotechnologies (Rio de Janeiro, RJ) and your identification and purity (>95%) was confirmed by HPLC-MS.

4.2.2 Preparation of BNC hydrogels

Gluconacetobacter hansenii, ATCC 23769 obtained from "Coleção de Cultura Tropical (CCT)", Fundação André Tosello, (Campinas, SP) was used to produce BNC hydrogels. G. hansenii was cultured in mannitol medium (25 $g \cdot L^{-1}$), yeast extract (5.0 $g \cdot L^{-1}$) and peptone (3.0 $g \cdot L^{-1}$), adjusted to pH 6.5 and sterilized. One hundred microliter of inoculum were added in mannitol agar plates. Mannitol agar plates were incubated at 26 °C for five days. Thirty single colonies were randomly selected and inoculated into 6 mL of mannitol medium. Subsequently, a solution composed by inoculum and mannitol medium (1:9) was stirred and transferred to 24 wells plates (1 mL/well). After four days of incubation, BNC hydrogels produced under static conditions at 26 °C were carefully removed and purified with 0.1 M NaOH solution at 50 °C for 24 h and finally rinsed with distilled water to pH 6.5.

4.2.3 Fabrication of BNC–IKVAV hydrogels

BNC hydrogels were oxidized with HNO_3/H_3PO_4-$NaNO_2$ following the procedure described by Kumar and Yang (2002) [46]. Briefly, a solution of nitric acid (68% v/v) and phosphoric acid (85% v/v) were prepared (2:1 ratio) and BNC hydrogels (50 samples) were submersed in 45 mL of the acid solution. Carefully, 0.63 g of sodium

nitrite was added and the solution was kept at room temperature during 24 h, in the absence of light. After that, BNC hydrogels were transferred to 0.2% (w/w) glycerol solution (15 min) to remove the residual part of the previous oxidative reaction. BNC hydrogels were finally washed with acetone and air-dried for 30 min at 60 °C. Oxidized BNC hydrogels were immersed in 45 mL of 0.02 M MES (4-morpholineethanesulfonic acid monohydrate) containing 0.01 M of EDC ((1-ethyl-3-(3-dimethylaminopropyl) carbodiimide) (pH 4.0–4.5), during 24 h at 4 °C [47]. Oxidized BNC, hydrogels were washed with deionized water and immersed in 20 mL of 0.1 $mg \cdot mL^{-1}$ IKVAV aqueous solution at 4 °C for at least 24 h. BNC–IKVAV hydrogels were washed with PBS buffer three times and rinsed with deionized water. Samples were lyophilized at -50 °C and sterilized by UV light during 30 min for in vitro tests.

4.2.4 Characterization of BNC–IKVAV hydrogels

4.2.4.1 Chemical characterization of BNC–IKVAV hydrogels

BNC and BNC–IKVAV hydrogels were chemically analyzed using Fourier Transformed Infrared Spectroscopy (FTIR). Infrared spectra were recorded on an Agilent spectrophotometer (model Carry 600), with a resolution of 4 cm^{-1}, in the range of 4000-600 cm^{-1}, using attenuated total reflectance.

4.2.4.2 Microstructural characterization of BNC–IKVAV hydrogels

Scanning electron microscopy (SEM) was performed to analyze the microstructure of BNC and BNC–IKVAV hydrogels surfaces. BNC and BNC–IKVAV hydrogels were characterized using a JEOL JSM-6390LV microscope operated at 10 kV. Prior to analyses, freeze-dried samples were cut into small pieces and coated with a thin layer of sputtered gold.

4.2.4.3 Characterization of the surface area, pore volume and distribution of pore diameter of BNC and BNC–IKVAV hydrogels

Nitrogen adsorption–desorption at 77 K was conducted with a liquid nitrogen trap according to the principle of static volumetric method for BNC and BNC–IKVAV hydrogels by a Quantachrome NovaWin version 10.01. The surface area (SA) was calculated by Brunauer-Emmett-Teller (BET) model and pore volume (PV) and distribution pore diameter (PD) were calculated by Barrett–Joyner–Halenda (BJH) model.

4.2.4.4 Detection of primary and secondary amines on BNC–IKVAV hydrogels

Ninhydrin assay, described by Moore and Stein (1968), was used to verify the presence of amine groups on the surface of BNC–IKVAV hydrogels [48]. Ninhydrin (4 g) were dissolved in 15 mL of DMSO and 5 mL of 4 M acetate buffer (pH 5.2) were added. Samples (1.91 cm^2) were submersed in a ninhydrin solution and incubated at 80 °C for 30 min protected from light. After 15 min of heating, 100 µL of ethanol 50% were added as stabilizing agent to the solution. Then the absorbance was measured at 570 nm. A standard curve of IKVAV was prepared to analyze the results.

4.2.5 Cell culture

Immortalized murine fibroblast cell line (L929) and immortalized human melanoma cells SK–MEL–28 were cultured in DMEM (Dulbecco's Modified Eagle's Medium) supplemented with 10% FBS and 1% penicillin/streptomycin. Immortalized human umbilical vein endothelial cells (HUVEC) were maintained in RPMI-1640 medium supplemented with 10% FBS, 1% penicillin/streptomycin. Cell cultures were maintained in a humidified CO2 (5% in air) incubator at 37 °C. All cells were cultured in culture plate until reaching 80% of confluence. Confluent cells were dissociated with trypsin, and centrifuged for 2-3 min. L929 cells were used between passages 16 and

18, HUVEC cells between passages 51 and 53 and SK–MEL–28 cells between 10 and 20.

4.2.6 Cytotoxicity assay

Cytotoxicity assay was performed with L929 murine fibroblast cell line cultured in direct contact with BNC and BNC–IKVAV hydrogels following ISO standard 10993-05 guidelines for direct testing of medical devices [49]. L929 cells were seeded in a 24 wells plate in a density of 9×10^3 cells·cm^{-2} during 24 h and they were kept in a humidified atmosphere containing 5% CO_2 at 37 °C. After incubation, BNC and BNC–IKVAV hydrogels were added into each well. At the end of 1, 3 and 7 days, samples and culture medium were removed and the adhered cells were rinsed with PBS three times. Metabolic activity was determined by mitochondrial activity through MTS [3-(4, 5-dimethylthiazol-2-yl)-5-(3-carboxymethoxyphenyl)-2-(4-sulfophenyl)-2H-tetrazolium] colorimetric assay from Promega Biotecnologia do Brasil, Ltda. (São Paulo, SP). MTS assay was performed according to the manufacturer's instructions. Three hundred and sixty microliters of culture medium and MTS (5:1) were added on each well of a 24 wells plate where L929 cells were adhered. Culture plates were kept in a humidified 5% CO_2 incubator at 37 °C protected of light during 2 h for the MTS reaction. The metabolic activity of L929 cells were quantified by Micro ELISA reader, at a wavelength of 490 nm.

4.2.7 Adhesion, proliferation and morphology of SK–MEL–28 cells on BNC and BNC–IKVAV hydrogels

SK–MEL–28 cells were seeded on top and bottom surfaces of BNC and BNC–IKVAV hydrogels in a density of 5.2×10^4 cells·cm^{-2}. After that, SK–MEL–28 cells were kept during 4 h to allow cell adhesion and during 1, 2, 3 and 7 days to evaluate cell proliferation. Cells were incubated at 37 °C with 5% of CO_2. A MTS assay kit was used to quantify the adhesion and proliferation of SK–MEL–28 cells over 7 days. MTS colorimetric assay was performed as previous described on Section 2.6.

To analyze cell behavior and morphology, SK–MEL–28 cells were stained with 4',6-diamidino-2-phenylindole dihydrochloride (DAPI) and Alexa Fluor 546 conjugated with phalloidin. SK–MEL–28 cells were previously fixed with 4% formaldehyde for 30 min and permeabilized with 0.1% Triton X-100 for 5 min at room temperature. Phalloidin and DAPI were used to stain F-actin and nuclei, respectively. Images were taken using a confocal laser scanning microscopy (CLSM) Leica Microsystems (model DMI6000 B). Morphology of adhered SK–MEL–28 cells on top surface and bottom surface of the hydrogels (BNC and BNC–IKVAV) were evaluated after 24 h of cultivation, and compared to SK–MEL–28 cells cultured on 2D culture plate under the same conditions.

4.2.8 Vasculogenic mimicry induction

SK–MEL–28 cells were seeded (10^5 cells·cm^{-2}) on bottom surface of BNC–IKVAV hydrogels and incubated for 24 and 48 h within a humidified incubator containing 5% of CO2 at 37 °C. As control, SK–MEL–28 cells were seeded on Geltrex® matrix (LDEV-Free Reduced Growth Factor Basement Membrane Matrix, Thermo Fisher Scientific). The performance of Geltrex® was tested with HUVEC cells prior to use as positive control. After 24 and 48 h of in vitro culture, SK–MEL–28 cells were fixed with 4% of formaldehyde for 30 min at room temperature. Phase contrast images were taken using an Olympus BX4 microscope (Olympus America Inc.). The WimTube software (Wimasis Image Analysis) was used to analyze and quantify the covered area, tube length, branching points and loops of vascular mimicry tube networks.

4.2.9 Statistical analysis

Statistical analysis were performed by the method one-way analysis of variance (ANOVA) with Tukey test. $P < 0.05$ was considered significant. The results were expressed as the mean ± standard error. All experiments were run in triplicate at two separated times.

4.3 RESULTS

4.3.1 Chemical immobilization and microstructural characterization of BNC and BNC–IKVAV hydrogels

BNC and BNC–IKVAV hydrogels were successfully synthesized and standardized for all assays. To immobilize the IKVAV peptide, BNC hydrogels were oxidized with HNO_3/H_3PO_4-$NaNO_2$ to convert the free hydroxyl groups of BNC to carboxyl groups. HNO_3/H_3PO_4–$NaNO_2$ mediated the oxidative reaction that was initiated by α-hydrogen atom abstracted from C6 of BNC by such odd-electron species of NO_2 and NO, giving as product BNC-COOH (Fig. 1a). The advantages of using HNO_3/H_3PO_4–$NaNO_2$ as oxidative agent of polysaccharides were related to the high selectivity and yield [46]. After activating the carboxyl groups of oxidized BNC hydrogels with EDC, IKVAV was covalently bonded onto the carboxyl now present in BNC hydrogels. The reaction between the amino groups of IKVAV and the carboxyl groups of BNC was represented in Figure 1b.

Figure 01. Immobilization reaction of IKVAV in BNC hydrogels. a) Oxidation process with HNO_3/H_3PO_4-$NaNO_2$ to convert the free hydroxyl groups of BNC to carboxyl groups, resulting in oxidized BNC (BNC-ox). b) Activation of the carboxyl groups present on the BNC-ox with EDC (coupling agent). Followed by the covalent reaction between active carboxyl groups on BNC-ox and the amine groups of the IKVAV peptide, resulting in BNC-IKVAV hydrogel.

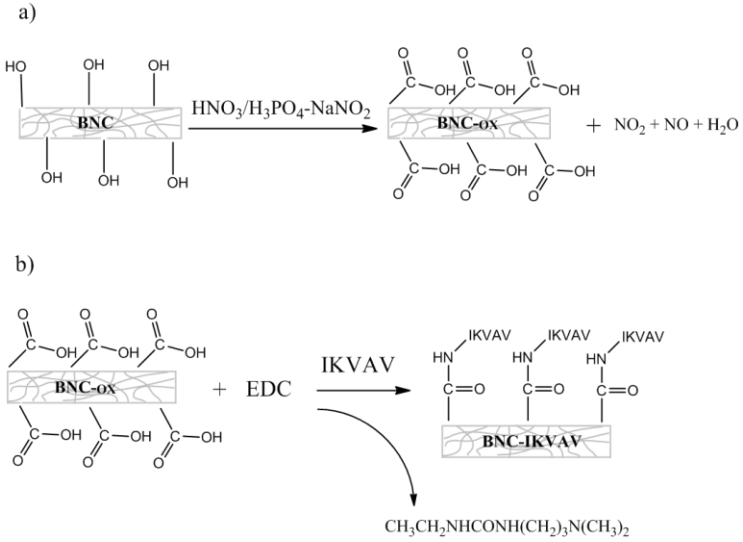

FTIR analysis showed the characteristic spectrum of BNC and BNC–IKVAV hydrogels which supports the effectiveness on the functionalization of BNC with the IKVAV peptide (Fig. 2). BNC FTIR spectrum showed characteristic bands of BNC, where the absorption band assigned to the hydroxyl group and hydrogen bond observed at 3345 cm^{-1} [50]. BNC–IKVAV FTIR spectrum showed a group of characteristic bands of amide I appeared in the 1623 cm^{-1}. An amide group in the L-sheet conformation gives rise to bands between approximately 1620 and 1640 cm^{-1} in the amide I region [50]. The absorption peaks between 2700–3000 cm^{-1} are characteristic bands of

NH_3^+, NH_2^+ or NH^+ stretchings. These results indicate the presence of IKVAV immobilized on BNC hydrogels.

Figure 2. FTIR spectroscopy of BNC and BNC-IKVAV. FTIR spectra of BNC with characteristic groups hydroxyl (OH) and alkanes (CH). BNC-IKVAV with characteristic groups amines (NH^+, NH_2^+, NH_3^+), amide I (N-C=O) and hydroxyl (OH).

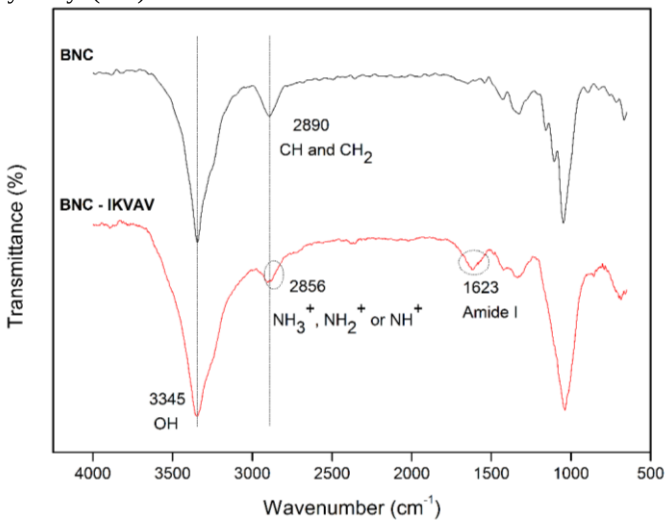

The microstructure of the bottom and top surfaces of BNC and BNC–IKVAV hydrogels were analyzed by SEM micrographs (Fig. 3). The microstructure of BNC hydrogels was characterized by 3D network structure characteristic. The bottom surface of BNC hydrogels were characterized by a 3D nanofiber network with random assembled nanofibers and interconnected pores (Fig. 3a). The top surface of BNC hydrogels were characterized by an entangled arrangement of nanofibers within no significant porous (Fig. 3b). SEM micrographs of the bottom surface of BNC–IKVAV hydrogels showed that the nanofibers kept randomly arranged containing some granules related to the peptide (IKVAV) immobilization over the nanofibers network (Fig. 3c). Similar granules were observed in a previous work [51] when collagen peptide was immobilized on dialdehyde BNC hydrogels. Those arrangements of

nanofibers and granules observed on the bottom surface of BNC–IKVAV hydrogels were not observed on the top surface of BNC–IKVAV. Top surface of BNC–IKVAV hydrogels kept the same fiber arrangement observed on the top surface of BNC hydrogels (Fig. 3d). Additionally, Brunauer-Emmett-Teller (BET) results showed that the immobilization of IKVAV altered pore volume (PV) and surface area (SA) of BNC hydrogels. SA and PV results were shown in Table 1. SA and PV of BNC–IKVAV hydrogels increased 25 % and 28 %, respectively, compared to BNC hydrogels. BNC and BNC–IKVAV hydrogels showed a similar distribution of pore size with diameters in a range of 3.4–30.3 nm to BNC and 3.3–28.5 nm to BNC–IKVAV, respectively.

Figure 3. SEM micrographs of BNC and BNC-IKVAV hydrogels. a) Bottom surface BNC hydrogel, b) Top surface BNC hydrogel, c) Bottom surface BNC-IKVAV hydrogel and d) Top surface BNC-IKVAV hydrogel.

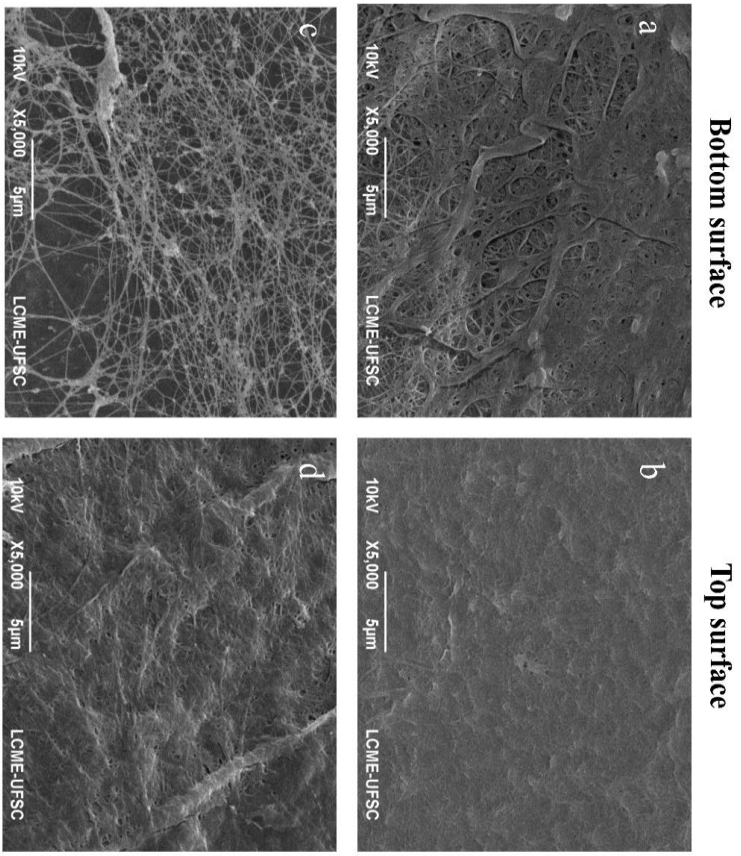

Table 1. Surface area (SA) and pore volume (PV) of BNC and BNC-IKVAV hydrogels.

Sample	TPV ($cm^3.g^{-1}$)	SSA ($m^2.g^{-1}$)
BNC	0.215	132.812
BNC-IKVAV	0.269	170.490

Amine groups were identified on the surfaces of BNC–IKVAV hydrogels by ninhydrin assay. Ninhydrin bound to amine groups present on the surface of the hydrogels produce a purple pigment that was detected by spectrophotometry at 570 nm. According to the standard curve, the equivalent amount of IKVAV immobilized on the BNC hydrogels was 18 $\mu g \cdot cm^{-2}$ (1.87% w/w). Our results showed an efficient immobilization of IKVAV when compared to results obtained by Liu et al. (2005) that used the same method to immobilize collagen on polyacrylonitrile (PAN) membranes. In that work they immobilized collagen in a density of 6.5 $\mu g \cdot cm^{-2}$ [47].

4.3.2 Cytotoxicity

BNC hydrogels have been defined in the literature as a no cytotoxic biomaterial for tissue engineering applications [52]. To assess if the immobilization of IKVAV peptide on BNC hydrogels could affect the cytotoxic potential of BNC hydrogels in mammalian cells we performed a cytotoxicity test. The results obtained by MTS assay showed that BNC and BNC–IKVAV hydrogels did not induce any cytotoxic response on L929 cells after 7 days of culture, following the guide to cytotoxicity tests in vitro for medical devices ISO 10993-5: 2009-[49]. After 1, 3 and 7 days of in vitro culture, BNC–IKVAV hydrogels improved the metabolic activity of L929 cells in 103%, 123% and 104%, respectively, compared to BNC hydrogels (100%) (Fig. 4).

Figure 4. Metabolic activity of L929 cells after direct contact with BNC and BNC-IKVAV during 7 days. * Significantly different, P<0.05.

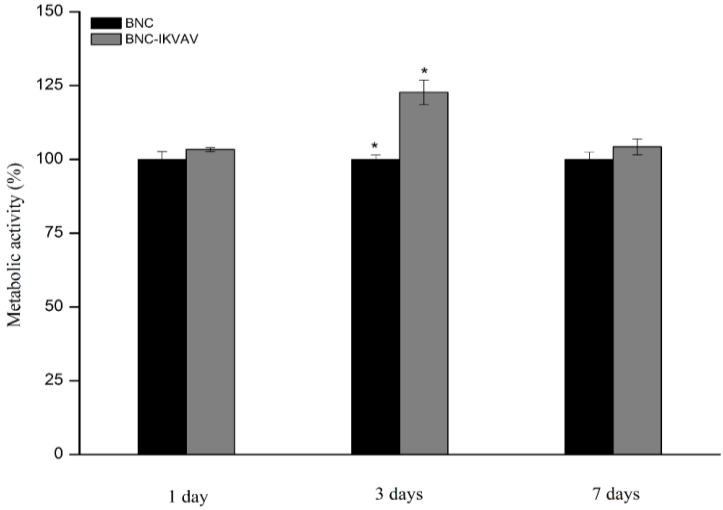

4.3.3 Adhesion, proliferation and morphology of SK–MEL–28 cells on BNC and BNC–IKVAV hydrogels

MTS assay was also used to determine the influence of the chemical and the microstructure surfaces of BNC and BNC–IKVAV hydrogels on SK–MEL–28 cells adhesion and proliferation after 4 h, 1, 2, 3 and 7 days (Fig. 5). After 4 h of culture, the metabolic activities of SK–MEL–28 cells increased when they were cultured on the bottom surface of BNC–IKVAV compared to the bottom surface of BNC. The results showed that in the early contact (4 h) between cells and hydrogel surfaces there were 85% more adherent SK–MEL–28 cells on the bottom surface of BNC–IKVAV, than on the same surface of BNC (100%). From 1, 2, 3 and 7 days, the metabolic activity of SK–MEL–28 cells increased when they were cultured on bottom surface of BNC–IKVAV compared to the bottom surface of BNC hydrogels. The increasing of metabolic activity of SK–MEL–28 cells were 55, 58, 20

and 272% for 1, 2, 3 and 7 days, respectively. SK–MEL–28 cells also adhered and proliferate more on the top surface of BNC–IKVAV compared to the top surface of BNC. In this case, the increasing of metabolic activities were 221, 65, 74, 98 and 132% to 4 h, 1, 2, 3 and 7 days, respectively. The top surface of BNC and BNC–IKVAV induced SK–MEL–28 cells proliferation more than the bottom surfaces of the same biomaterials. After 1 day of culture there were no statistic differences on cell adhesion and proliferation comparing the bottom surface of BNC and top surface of BNC. An increasing of cell proliferation on the top surface of BNC in comparison to the bottom surface of BNC hydrogels was of 12, 13 and 125% considering 2, 3 and 7 days, respectively. Additionally, the top surface of BNC–IKVAV increased the tumor cells proliferation compared to the bottom surface of BNC–IKVAV (21, 22, 87 and 40% for 1, 2, 3 and 7 days of cultivation, respectively).

Figure 5. Adhesion and proliferation of SK–MEL–28 cells cultured on top and bottom surfaces of BNC and BNC–IKVAV hydrogels during 7 days of in vitro culture.

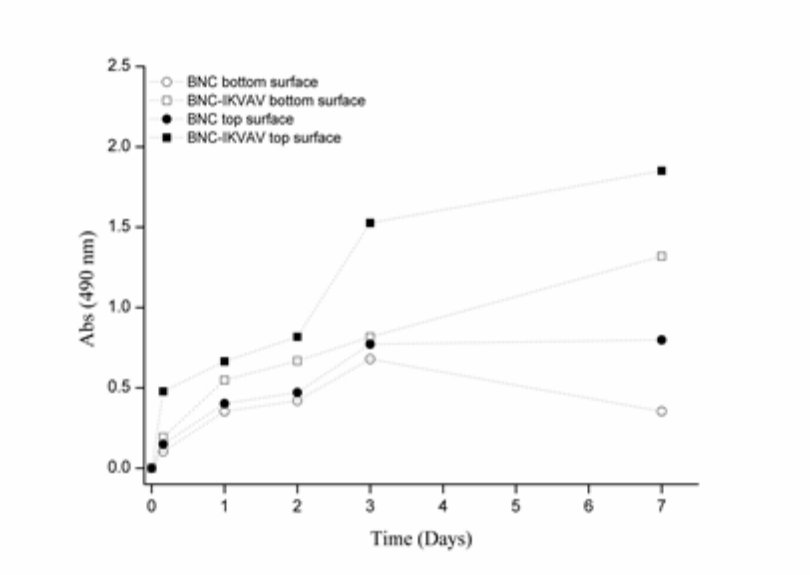

The cells–hydrogels interaction was investigated by confocal microscopy after 4 h, 1, 2, 3 and 7 days. SK–MEL–28 cells were seeded on both surfaces of BNC and BNC–IKVAV hydrogels. The presence of single cells was predominant during the early stages (4 h) of in vitro culture on the bottom surface of the BNC (Fig. 6a). On the top surface of BNC hydrogels, small clusters of SK–MEL–28 cells had already been formed after 4 h of culture (Fig. 6f). SK–MEL–28 cells adhered over both surfaces of BNC. However, the top surface of BNC had a greater number of proliferative cells (Fig. 6g-j) compared to the bottom surface of BNC (Fig.6b-e). SK–MEL–28 cells cultured on both surfaces of BNC organized themselves as tumor-like masses or tumoroids. SK–MEL–28 cells formed tight cellular tumoroids ranging 30 to 100 µm of diameter when cultured on BNC surfaces. The diameter average presented was the average of 20 tumoroids/day. Tumoroids numbers were counted from full images considering the total surface of each hydrogel. Rounded aggregates of size ≥ 30 µm were counted as tumoroids. Tumoroids numbers were estimated from full confocal images of SK–MEL–28 cultured on BNC hydrogels surface considering the total surface of each hydrogel. Rounded aggregates with size ≥ 30 µm were counted as tumoroids.

SK–MEL–28 cells showed a completely different behavior when they were cultured on BNC–IKVAV. After 4 h of culture, adherent SK–MEL–28 cells showed rounded shape, typical of the early stages of the cellular adhesion, without the formation of clusters on both surfaces of BNC–IKVAV (Fig. 6k, p). On the top surface of BNC–IKVAV there were more adherent SK–MEL–28 cells (Fig. 6q-t) compared to the bottom surface of the same hydrogel (Fig. 6l-o). SK–MEL–28 cells proliferate on the top surface of BNC–IKVAV maintaining the rounded shape over 7 days of in vitro culture. From 3 to 7 days of culture it was possible to observe multilayers of SK–MEL–28 cells on the top surface of BNC–IKVAV (Fig. 6s, t). SK–MEL–28 cells cultured on the bottom surface of BNC–IKVAV organize themselves in a network arrangement with elongated phenotype from 24 h to 3 days of in vitro culture (Fig.6l-n). On the second and third days, those cells were self-organized and elongated and they maintained cell-cell contact, building a secondary mechanism for tumor re-vascularization, known as vascular mimicry (Fig. 6m, n). SK–MEL–28 cells remained proliferative

until day 7 of culture when they became more connected (higher density) and shape rounded (Fig. 6o).

Figure 6. CLSM images of SK–MEL–28 cells cultured on top and bottom surfaces of BNC and BNC–IKVAV hydrogels. SK–MEL–28 cells were stained with Alexa Fluor 546 conjugated to phalloidin (red) and DAPI (blue). SK–MEL–28 cells were cultured on bottom and top surface of BNC and BNC-IKVAV hydrogels during 4h, 1d, 2d, 3d and 7d.

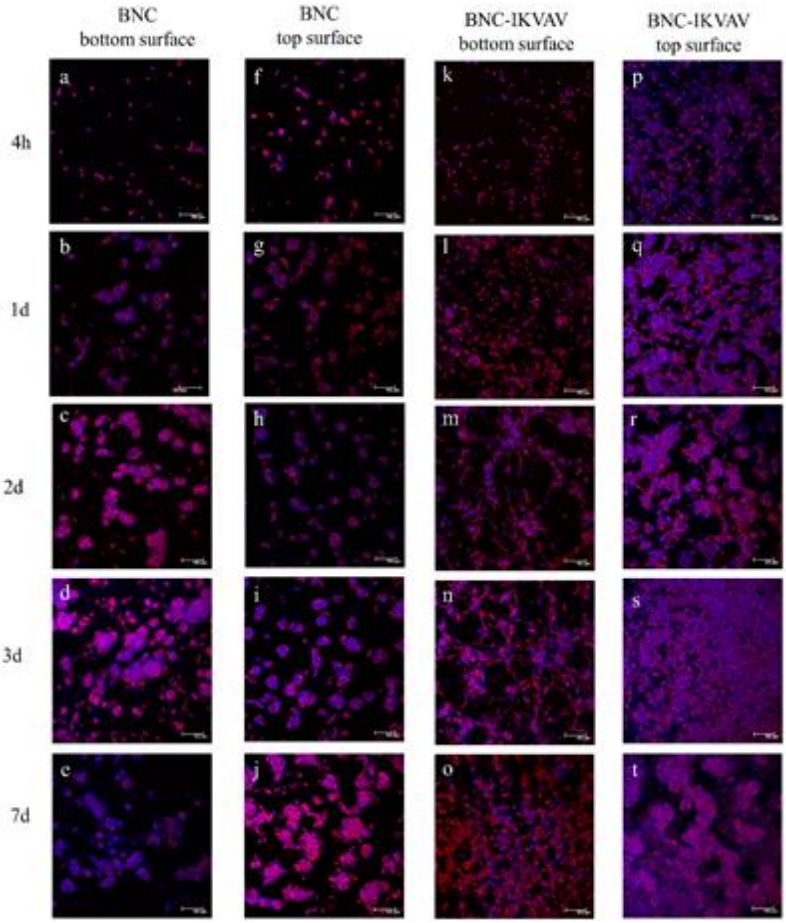

SK–MEL–28 cells morphology, after 24 hours of culture on BNC and BNC–IKVAV were analyzed by confocal microscopy (CLSM) (Fig. 7). SK–MEL–28 cells cultured on both surfaces of BNC showed similar rounded morphology (clusters). The cell clusters formed presented rounded morphology with several blebs on their plasmatic membrane (Fig. 7a, b) which could be related to an invasive stage of tumor cells progression. Cell-cell adhesion in was observed on tumoroids formed on BNC hydrogels. SK–MEL–28 cells cultured on the top surface of BNC–IKVAV showed rounded morphology with blebs or protusions formation after 24h of culture (Fig.7d). However, as SK–MEL–28 cells were not organized in cell clusters or tumoroids and their morphology has been associated with amoeboid movements [53]. When SK–MEL–28 cells were seeded on the bottom surface of BNC–IKVAV, those cells presented an elongated shape with cytoskeletal protrusions known as invapodia (Fig. 7c). The presence of invapodia has been related with mesenchymal movements, other form of plasticity of the invasive tumor cells. However, the formation of blebs was also present in SK–MEL–28 cells cultured on bottom surface of BNC–IKVAV. SK–MEL–28 cells grown on culture plates and showed elongated shape without any protuberances on their plasmatic membrane (Fig. 7e), typical morphology of melanoma cells when cultured on 2D culture.

Figure 7. CLSM images of SK–MEL–28 cells morphology cultured during 24h on a) bottom surface of BNC hydrogels, b) top surface of BNC hydrogels, c) bottom surface of BNC–IKVAV hydrogels, d) top surface of BNC–IKVAV hydrogels and e) 2D-tissue culture plate. Red arrows indicate protuberances on the SK–MEL–28 cells cytoplasm: a, c and d indicate blebs and b indicate blebs and invapodia. SK–MEL–28 cells were stained with Alexa Fluor 546 conjugated with phalloidin (red) and DAPI (blue).

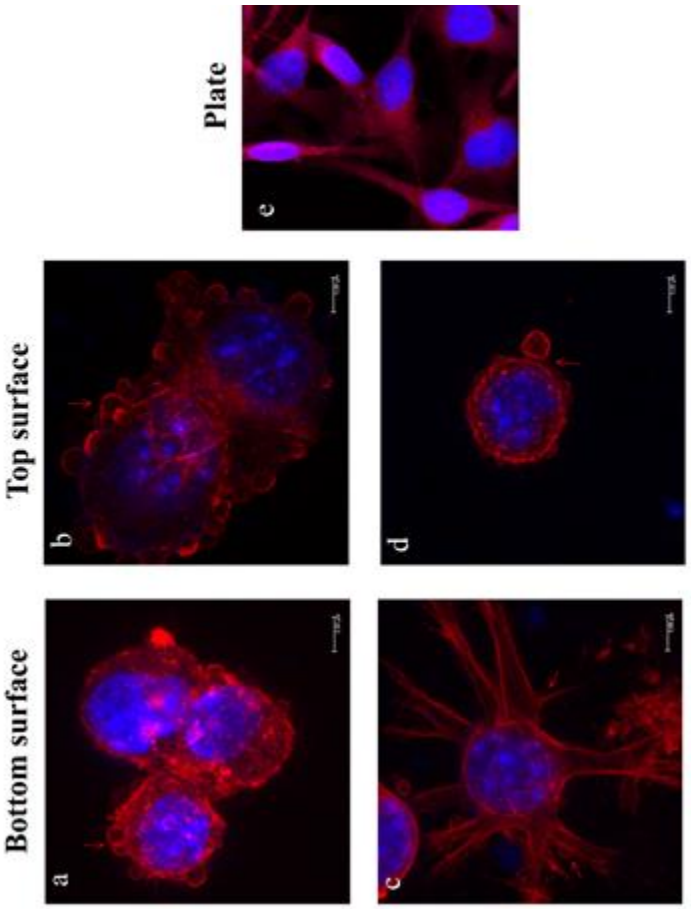

4.3.4 Vasculogenic mimicry induction

SK–MEL–28 cells cultured on the bottom surface of the BNC–IKVAV were able to interconnect their selves on networks. When 10^5 cells·cm^{-2} SK–MEL–28 cells were seeded on the bottom surface of BNC–IKVAV, they were able to form well–established networked like-endothelial vessels. After 24 h of in vitro culture, SK–MEL–28 cells induced an alignment with phenotype characteristic of endothelial cells on tubulogenesis process, with the presence of tip and stalk cells (Fig. 8) and the development of branching points and loops (Fig. 9).

Figure 8. Phase contrast images of SK–MEL–28 cells in the vascular mimicry n formation. SK–MEL–28 cells cultured on the bottom surface of BNC–I hydrogels during 24h. Red arrows indicate tip cells. Stalk cells were signali rings. Scale bars represent 100 µm.

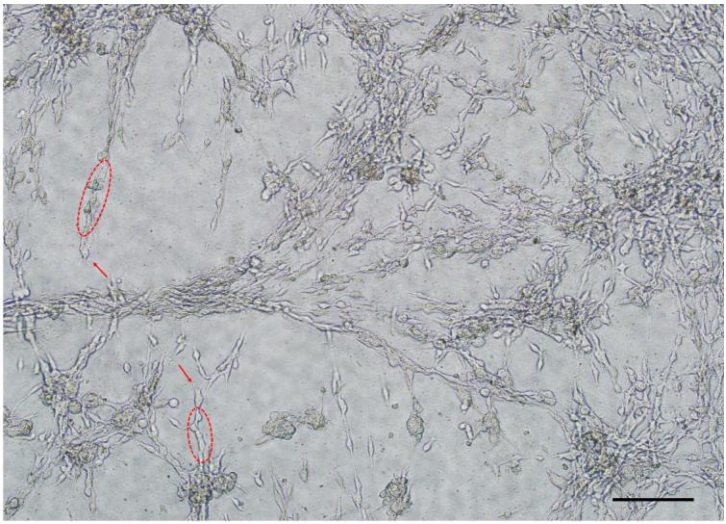

Figure 9. Phase contrast images of SK–MEL–28 cells in the vascular mimicry network formation. SK–MEL–28 cells cultured on the bottom surface of BNC–IKVAV hydrogels during 24h. Red dots indicate branching points and the loops are represented by rings. Scale bars represent 100 µm.

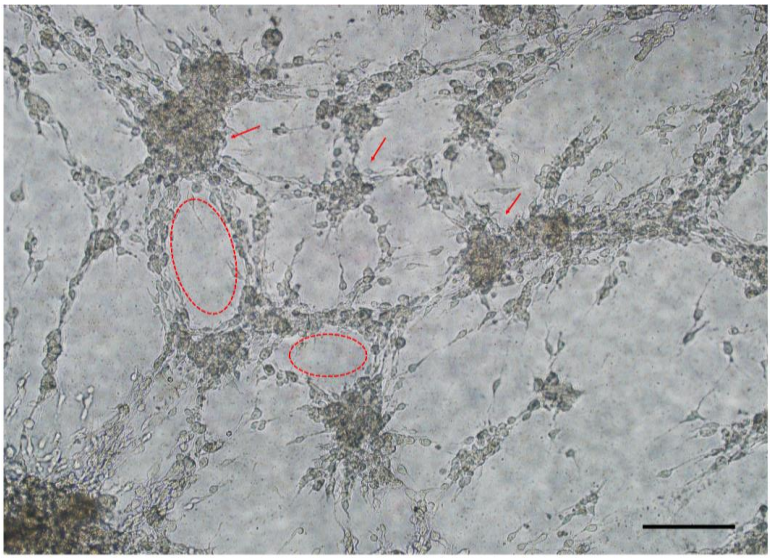

When SK–MEL–28 cells were culture on Geltrex®, a commercial ECM, they were not able to form a well-organized vascular network, forming badly finished tubes and tumoroids. Unlike, Geltrex® was able to induce HUVEC cells tubulogenesis (Fig. 10a), but not vasculogenic mimicry by SK–MEL–28 cells (Fig. 10b), as observed on the bottom surface of BNC–IKVAV (Fig. 10c). Vasculogenic mimicry network formed on the bottom surface of BNC-IKVAV showed 373 ± 28 tubes, 196 ± 13 branching points and 63 ± 5 loops after 24 h of culture; and 458 ± 43 tubes, 246 ± 18 branching points and 87 ± 18 loops after 48 h of culture (Fig. 11a, b). However, there were no

statistical differences ($P<0.05$) in the analyzed parameters comparing 24h to 48h of SK-MEL-28 vasculogenic mimicry network formation.

Figure 10. Phase contrast images of a) SK–MEL–28 cells cultured on the bottom surface of BNC–IKVAV hydrogels, b) SK–MEL–28 cells cultured on Geltrex® matrix, and c) HUVEC cells cultured on Geltrex® matrix, as positive control. SK–MEL–28 and HUVEC cells were cultured during 24 h on the referred materials. Scale bars represent 100 µm.

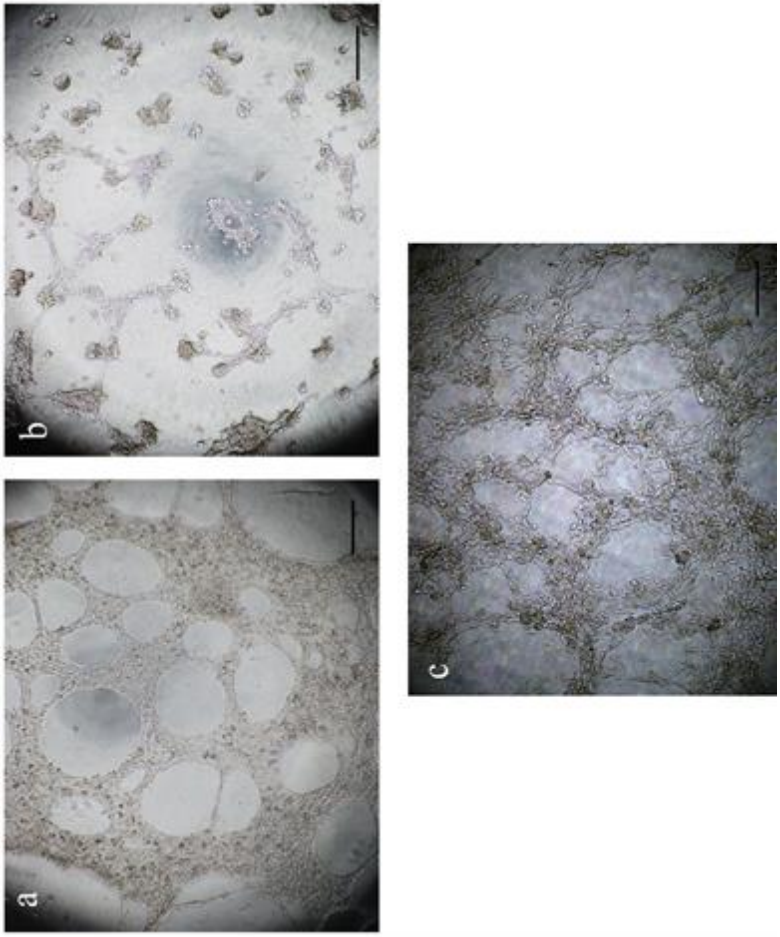

Figure 11. Phase contrast images of: a and b) SK–MEL–28 cells cultured on the bottom surface of BNC–IKVAV hydrogels, b and c) SK–MEL–28 cells cultured on the bottom surface of BNC–IKVAV hydrogels analyzed by WimTube software. SK–MEL–28 and cells were cultured during 24 h. Scale bars represent 50 µm.

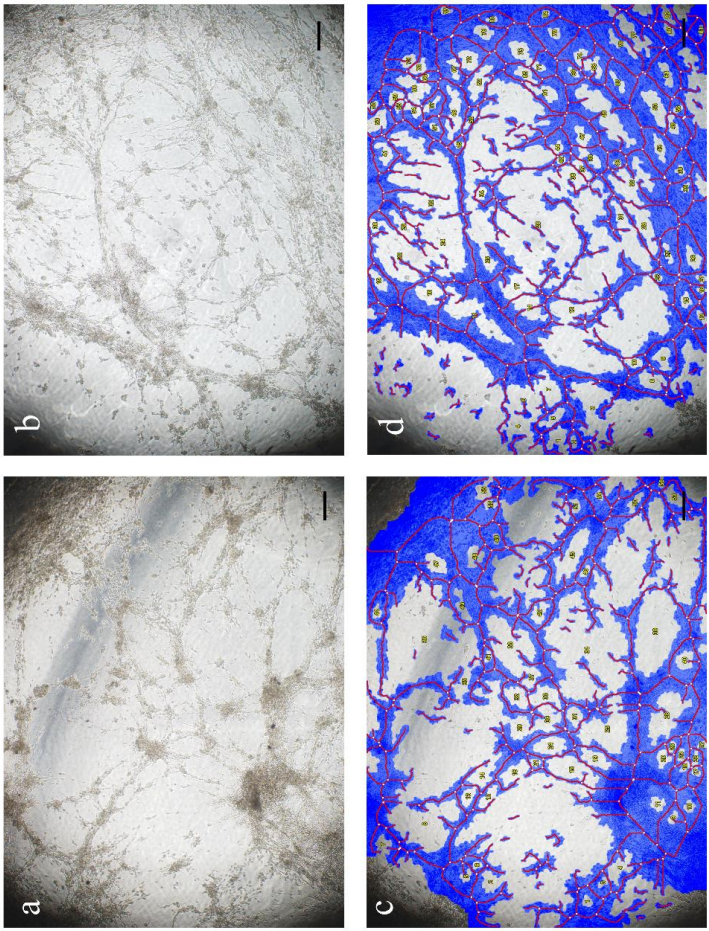

4.4 DISCUSSION

The plasticity of tumor cells has been related as dependent of the 3D microenvironment where those cells are growing [54]. Tissue microstructure and biochemical composition are important factors that have determined the tumor behavior and progression [55, 56]. Several efforts have been done in the development of an artificial and reproductive 3D microenvironment that resembles tumor ECM to understand the strategy of the tumor progression that requires blood vessels to access oxygen and nutrients and also to become invasive and metastatic. In this context, we successfully developed a 3D platform based on BNC immobilized with IKVAV peptide that simulated the tumor ECM inducing the plasticity of SK–MEL–28 cells present on aggressive cancers. It has been well established in the literature that tumor cells-ECM interactions cannot be replicated using 2D culture methods and the effect of antitumor drugs should be tested on 3D culture platforms [57].

In this work, IKVAV peptide was chemically immobilized on BNC hydrogels and performed the physicochemical characterization of a novel BNC–IKVAV hydrogels was also platform performed. There were particular characteristics related to the chemistry and microstructure of the top and bottom surfaces of BNC and BNC–IKVAV that resembled the in vivo microenvironment in different plasticities of tumor development. SK–MEL–28 cells were able to adhere and acquire phenotypes of tumor cell invasiveness on the both surfaces (top and bottom) of BNC and BNC–IKVAV hydrogels.

SK–MEL–28 cells were more proliferative and metabolically active when they were cultured on BNC–IKVAV than on BNC. Our results showed an improvement of twice in cell adhesion, comparing the bottom surfaces of BNC–IKVAV to BNC. On the top surface, the increasing on cell adhesion was three times higher when SK–MEL–28 cells were cultured on BNC–IKVAV compared to BNC. In a previous work [58], IKVAV have been absorbed on BNC hydrogels to improve the adhesiveness, but those authors do not immobilized the peptide. Pertile and co-authors (2012) improved 100% the adhesion of pheochromocytoma rat cells on BNC adsorbed with IKVAV compared

to pure BNC hydrogels. However, on that work, the authors not mentioned which surface of BNC hydrogels were used to seed rat cells [58].

Our results also showed that the immobilization of IKVAV peptide influenced SK–MEL–28 proliferation. SK–MEL–28 cells proliferate higher on the BNC-IKVAV that BNC hydrogels. When comparing the same hydrogel, the top surface of BNC-IKVAV provided greater proliferation than the bottom surface of BNC-IKVAV.

Recent reports have claimed that differences on the microstructure of the BNC hydrogels interfere directly on cell behavior. Berti and colleagues (2013) showed that HUVEC cells cultured on top and bottom surface of BNC hydrogels showed distinct behaviors [31]. Christopher et al. (2011) reported low adherence and proliferation when breast cancer cells were cultured on BNC hydrogels. The authors suggested that modifications on BNC surface would be necessary to improve the adhesion of tumor cells [59]. Our study corroborates the idea that the biomaterial microstructure determines cell behavior and it should be an important parameter to be considered on tissue engineering developments. Furthermore, our results suggest that the bottom surface of BNC–IKVAV induced SK–MEL–28 cells follow amoeboid and/or mesenchymal pathways. Particularly, SK–MEL–28 cells form vascular networks, known as tumor cell vascular mimicry [14], after 24 h of in vitro culture on the bottom surface of BNC–IKVAV.

In tissue engineering and regenerative medicine applications, hydrogels have been highlighted because they hold a highly porous microstructure which provides an interconnected surface area that allows cell ingrowth [60, 61]. Porous surfaces have been related to cell and induction of neovascularization in 3D microenvironments [62]. That means that important parameters, such as pore size, pore volume, pore distribution, and surface area should be considered in the design of tissue engineering scaffold constructions. BNC and BNC–IKVAV, with pores size ranging from 3.39 to 30.34 nm, may be classified as mesoporous hydrogels [63]. The differences on the microstructure of BNC hydrogels surfaces (top and bottom) have been previously reported and SEM results reinforced those findings [64–66]. BNC–IKVAV showed an increase of 25% on surface area when compared to BNC.

This is in accordance with Joo et al., (2006) work that reported an increase on the surface area of cellulose performing the same oxidation reaction (HNO_3/H_3PO_4-$NaNO_2$) [67].

Cancer cells have adapted their cell behavior on different microstructures assuming several morphologies and migration characteristics to move during the first stage of metastasis, cell invasion [7]. The development of a 3D platform that mimics tumor microenvironment, inducing tumor cell plasticity, is desired to identification studies of novel anticancer targets. Tumor cells migration and invasiveness has been classified based on their morphology on 3D hydrogels [53]. Generally, the invasiveness requires cell-cell adhesion [11] that usually has been related to a small cell clusters as observed on tumoroids formed on BNC hydrogels. SK–MEL–28 cells assumed tumoroid characteristics when cultured on the two surfaces of the BNC hydrogels, showing that on that microstructure the cell-cell interaction was greater than the cell-hydrogel interaction. After 24 h of culture, SK–MEL–28 tumoroids showed a typical morphology of amoeboid movements in collective invasion, containing several blebs around. In addition, the SK–MEL–28 tumoroids showed ideal size (30-100 μm) for use as cancer drugs screening platform [68–70]. When cells were cultured on top surface of BNC–IKVAV, they also showed rounded shape containing several blebs around them, typical mechanism of amoeboid movements in singular invasion. Unlike, SK–MEL–28 cells cultured on the bottom surface of BNC–IKVAV showed elongated morphology, typical of the mesenchymal movement of tumor invasion, In addition, cells with rounded shape and blebs were present on the bottom surface of BNC-IKVAV. Thus, SK–MEL–28 movements presented on the bottom surface of BNC–IKVAV were not purely mesenchymal, but also amoeboid. SK–MEL–28 cells behavior when cultured on 2D culture plates were completely different from their behavior on BNC and BNC–IKVAV hydrogels. Besides, our findings further support the concept that this 3D tumor platform mimics the in vivo tumor microenvironment.

SK–MEL–28 cells behavior were characteristic of vasculogenic mimicry [13] when cultivated on the bottom surface of BNC-IKVAV. After 24 h, SK–MEL–28 cells were aligned and formed networks

similar to endothelial cells on angiogenesis. SK–MEL–28 cells with similar shape and behavior of endothelial cells in angiogenesis process (tip and stalk cells, loops and branching points) were also present. We used Geltrex® as a positive control to perform our experiment. However, Geltrex® was not able to induce vasculogenic mimicry on SK–MEL–28 cells. We compared vascular mimicry networks formed by SK–MEL–28 after 24 and 48 h of culture on the bottom surface of BNC–IKVAV and quantified their main characteristics of vascular tube formation, such as number of tubes, branching points and loops (the usual characteristics quantified in the tubulogenesis assays). We found no significant differences between the number of tubes, branching points or loops formed after 24 and 48 h of culture on bottom surface of BNC–IKVAV. These results suggest that 24 h of SK–MEL–28 cells culture would be enough to the evaluation of anticancer drug test against vasculogenic mimicry using the bottom surface of BNC–IKVAV hydrogel platform. Our results are very similar to those found in the literature for melanoma cells cultured on Matrigel® forming vasculogenic mimicry networks [22, 34, 71]. Commercial ECM, such as Matrigel®, are chemically complex, containing growth factors, proteins and other components [20]. BNC–IKVAV hydrogels contain just one protein (laminin) though reassembling a competent ECM. We showed that laminin peptide associated with the particular microstructure of BNC hydrogels were able to induce vascular mimicry on the invasive human cancer cell. These results matched with the biological functions of laminin peptide, IKVAV, mentioned in the literature, as a peptide that improves adhesion and proliferation of cancer cells through the stimulation of tumor growth factor to achieve metastasis through vasculogenic mimicry [36], [72]–[74]. This suggests that the biological properties of IKVAV were kept after the immobilization on the bottom surface of BNC hydrogels. In addition, the immobilization of IKVAV peptide might be more effective on the bottom surface of BNC than on the top surface of BNC hydrogels.

We did not find other works in the literature proposing such to construct an ideal 3D environment to achieve vasculogenic mimicry for anticancer test platform. Our work is pioneering in the development of a vascular mimicry 3D platform. Future work will test the efficiency of BNC–IKVAV in the screening of anti-tumor drugs on vasculogenic

mimicry events. Tumor cells involved in vascular mimicry have been related as non sensible to angiogenesis inhibitors [75]. BNC–IKVAV hydrogels is an alternative in the discovery of effective cancer drugs able to block the vasculogenic mimicry process. Here, we developed a chemically well-defined vascular mimicry 3D platform based on BNC–IKVAV that may be used to study more than one type of tumor cell plasticity hydrogels.

4.5 CONCLUSION

IKVAV peptide was chemically immobilized on BNC hydrogels. SK–MEL–28 cells behavior were dependent of the microstructure and chemical composition. BNC and BNC–IKVAV hydrogels induced the plasticity of human melanoma (SK–MEL–28) cells. SK–MEL–28 cells cultured on top and bottom surfaces of BNC hydrogels formed tumoroids with rounded morphology of tumor cells similar to what have been found in a collective tumor cells invasion mechanism. When SK–MEL–28 cells were cultured on top surface of BNC–IKVAV, they showed rounded morphology containing blebs on their plasmatic membranes which were related to amoeboid movements found in tumor cell invasion. SK–MEL–28 cells vascular mimicry was induced when they were cultured on the bottom surface of BNC–IKVAV hydrogels. SK–MEL–28 cells in different mechanism of invasiveness plasticity were observed on BNC and BNC–IKVAV hydrogels. The proposed 3D platforms could be used as an alternative to development of customized melanoma anticancer drugs screening.

4.6 REFERENCES

[1] D. Schadendorf, D. E. Fisher, C. Garbe, J. E. Gershenwald, J.-J. Grob, A. Halpern, M. Herlyn, M. a. Marchetti, G. McArthur, A. Ribas, A. Roesch, and A. Hauschild, “Melanoma,” *Nat. Rev. Dis. Prim.*, no. April, p. 15003, 2015.

[2] World Health Organization., “How commom is skin cancer?,” 2016. [Online]. Available: http://www.who.int/uv/faq/skincancer/en/index1.html. [Accessed: 02-Jul-2016].

[3] S. Valastyan and R. A. Weinberg, “Tumor metastasis: Molecular insights and evolving paradigms,” *Cell*, vol. 147, no. 2. pp. 275–292, 2011.

[4] T. A. Martin, L. Ye, A. J. Sanders, J. Lane, and W. G. Jiang, “Cancer Invasion and Metastasis: Molecular and Cellular Perspective,” *Metastatic Cancer: Clinical and Biological Perspectives*, 2013. [Online]. Available: http://www.ncbi.nlm.nih.gov/books/NBK164700/?report=classic.

[5] J. H. Tsai and J. Yang, “Epithelial-mesenchymal plasticity in carcinoma metastasis,” *Genes and Development*, vol. 27, no. 20. pp. 2192–2206, 2013.

[6] J. L. Orgaz and V. Sanz-Moreno, “Emerging molecular targets in melanoma invasion and metastasis,” *Pigment Cell and Melanoma Research*, vol. 26, no. 1. pp. 39–57, 2013.

[7] P. Friedl and S. Alexander, “Cancer invasion and the microenvironment: Plasticity and reciprocity,” *Cell*, vol. 147, no. 5. pp. 992–1009, 2011.

[8] K. Wolf, I. Mazo, H. Leung, K. Engelke, U. H. Von Andrian, E. I. Deryugina, A. Y. Strongin, E. B. Br??cker, and P. Friedl, “Compensation mechanism in tumor cell migration: Mesenchymal-amoeboid transition after blocking of pericellular proteolysis,” *J. Cell Biol.*, vol. 160, no. 2, pp. 267–277, 2003.

[9] J. Marshall, “Transwell invasion assays,” *Methods Mol. Biol.*, vol. 769, pp. 97–110, 2011.

[10] K. I. Hulkower and R. L. Herber, “Cell migration and invasion assays as tools for drug discovery,” *Pharmaceutics*, vol. 3, no. 1. pp. 107–124, 2011.

[11] A. a Khalil and P. Friedl, “Determinants of leader cells in collective cell migration.,” *Integr. Biol. (Camb).*, vol. 2, no. 11–12, pp. 568–574, 2010.

[12] A. J. Maniotis, R. Folberg, A. Hess, E. A. Seftor, L. M. Gardner, J. Pe’er, J. M. Trent, P. S. Meltzer, and M. J. Hendrix, “Vascular channel formation by human melanoma cells in vivo and in vitro: vasculogenic mimicry,” *Am J Pathol*, vol. 155, no. 3, pp. 739–752, 1999.

[13] R. Folberg, M. J. Hendrix, and a J. Maniotis, “Vasculogenic mimicry and tumor angiogenesis.,” *Am. J. Pathol.*, vol. 156, no. 2, pp. 361–381, 2000.

[14] R. Folberg and A. J. Maniotis, “Vasculogenic mimicry,” *APMIS*, vol. 112, no. 7–8. pp. 508–525, 2004.

[15] H. Yamaguchi, J. Wyckoff, and J. Condeelis, “Cell migration in tumors,” *Current Opinion in Cell Biology*, vol. 17, no. 5 SPEC. ISS. pp. 559–564, 2005.

[16] C. Decaestecker, O. Debeir, P. Van Ham, and R. Kiss, “Can anti-migratory drugs be screened in vitro? A review of 2D and 3D assays for the quantitative analysis of cell migration,” *Medicinal Research Reviews*, vol. 27, no. 2. pp. 149–176, 2007.

[17] C. M. Nelson and M. J. Bissell, “Modeling dynamic reciprocity: Engineering three-dimensional culture models of breast architecture, function, and neoplastic transformation,” *Seminars in Cancer Biology*, vol. 15, no. 5 SPEC. ISS. pp. 342–352, 2005.

[18] R. Z. Lin and H. Y. Chang, “Recent advances in three-dimensional multicellular spheroid culture for biomedical research,” *Biotechnology Journal*, vol. 3, no. 9–10. pp. 1172–1184, 2008.

[19] L. C. Kimlin, G. Casagrande, and V. M. Virador, “In vitro three-dimensional (3D) models in cancer research: an update,” *Mol Carcinog*, vol. 52, no. 3, pp. 167–182, 2013.

[20] H. K. Kleinman and G. R. Martin, “Matrigel: Basement membrane matrix with biological activity,” *Semin. Cancer Biol.*, vol. 15, no. 5 SPEC. ISS., pp. 378–386, 2005.

[21] C. S. Hughes, L. M. Postovit, and G. A. Lajoie, “Matrigel: a complex protein mixture required for optimal growth of cell culture.,” *Proteomics*, vol. 10, no. 9, pp. 1886–1890, 2010.

[22] R. a. Francescone III, M. Faibish, and R. Shao, “A Matrigel-Based Tube Formation Assay to Assess the Vasculogenic Activity of Tumor Cells,” *J. Vis. Exp.*, no. 55, pp. 2–5, 2011.

[23] C. S. Hughes, L. Radan, D. Betts, L. M. Postovit, and G. A. Lajoie, “Proteomic analysis of extracellular matrices used in stem cell culture,” *Proteomics*, vol. 11, no. 20, pp. 3983–3991, 2011.

[24] I. El-Sherbiny and M. Yacoub, “Hydrogel scaffolds for tissue engineering: Progress and challenges,” *Glob. Cardiol. Sci. Pract.*, vol. 2013, no. 3, pp. 316–42, 2013.

[25] K.-L. Ou and H. Hosseinkhani, “Development of 3D in Vitro Technology for Medical Applications,” *Int. J. Mol. Sci.*, vol. 15, no. 10, pp. 17938–17962, 2014.

[26] D. Klemm, F. Kramer, S. Moritz, T. Lindström, M. Ankerfors, D. Gray, and A. Dorris, “Nanocelluloses: A new family of nature-based materials,” *Angewandte Chemie - International Edition*, vol. 50, no. 24. pp. 5438–5466, 2011.

[27] Y. Cao, M. R. Davidson, A. J. O’Connor, G. W. Stevens, and J. J. Cooper-White, “Architecture control of three-dimensional polymeric scaffolds for soft tissue engineering. I. Establishment and validation of numerical models,” *J. Biomed. Mater. Res. - Part A*, vol. 71, no. 1, pp. 81–89, 2004.

[28] A. Curtis and C. Wilkinson, “Topographical control of cells,” *Biomaterials*, vol. 18, no. 24. pp. 1573–1583, 1997.

[29] C. S. Chen, M. Mrksich, S. Huang, G. M. Whitesides, and D. E. Ingber, “Geometric control of cell life and death.,” *Science*, vol. 276, no. 5317, pp. 1425–1428, 1997.

[30] W. Borzani and S. J. De Souza, “Mechanism of the film thickness increasing during the bacterial production of cellulose on non-agitaded liquid media,” *Biotechnol. Lett.*, vol. 17, no. 11, pp. 1271–1272, 1995.

[31] F. V. Berti, C. R. Rambo, P. F. Dias, and L. M. Porto, “Nanofiber density determines endothelial cell behavior on hydrogel matrix,” *Mater. Sci. Eng. C*, vol. 33, no. 8, pp. 4684–4691, 2013.

[32] D. Klemm, D. Schumann, U. Udhardt, and S. Marsch, “Bacterial synthesized cellulose - Artificial blood vessels for microsurgery,” *Prog. Polym. Sci.*, vol. 26, no. 9, pp. 1561–1603, 2001.

[33] J. Zhu and R. E. Marchant, “Design properties of hydrogel tissue-engineering scaffolds.,” *Expert Rev. Med. Devices*, vol. 8, no. 5, pp. 607–26, 2011.

[34] M. J. C. Hendrix, E. A. Seftor, A. R. Hess, and R. E. B. Seftor, “Vasculogenic mimicry and tumour-cell plasticity: lessons from

melanoma.," *Nat. Rev. Cancer*, vol. 3, no. 6, pp. 411–21, 2003.

[35] J. Kruegel and N. Miosge, "Basement membrane components are key players in specialized extracellular matrices," *Cellular and Molecular Life Sciences*, vol. 67, no. 17. pp. 2879–2895, 2010.

[36] M. Nomizu, B. S. Weeks, C. A. Weston, W. H. Kim, H. K. Kleinman, and Y. Yamada, "Structure-activity study of a laminin ??1 chain active peptide segment Ile-Lys-Val-Ala-Val (IKVAV)," *FEBS Lett.*, vol. 365, no. 2–3, pp. 227–231, 1995.

[37] M. Yamada, Y. Kadoya, S. Kasai, K. Kato, M. Mochizuki, N. Nishi, N. Watanabe, H. K. Kleinman, Y. Yamada, and M. Nomizu, "Ile-Lys-Val-Ala-Val (IKVAV)-containing laminin ??1 chain peptides form amyloid-like fibrils," *FEBS Lett.*, vol. 530, no. 1–3, pp. 48–52, 2002.

[38] B. Li, T. Qiu, P. Zhang, X. Wang, Y. Yin, and S. Li, "IKVAV regulates ERK1/2 and Akt signalling pathways in BMMSC population growth and proliferation," *Cell Prolif.*, vol. 47, no. 2, pp. 133–145, 2014.

[39] B. Wu, Q. Zheng, Y. Wu, X. Guo, and Z. Zou, "Effect of IKVAV peptide nanofiber on proliferation, adhesion and differentiation into neurocytes of bone marrow stromal cells," *J. Huazhong Univ. Sci. Technol. - Med. Sci.*, vol. 30, no. 2, pp. 178–182, 2010.

[40] D. S. Grant, J. L. Kinsella, R. Fridman, R. Auerbach, B. a Piasecki, Y. Yamada, M. Zain, and H. K. Kleinman, "Interaction of endothelial cells with a laminin A chain peptide (SIKVAV) in vitro and induction of angiogenic behavior in vivo.," *J. Cell. Physiol.*, vol. 153, no. 3, pp. 614–25, 1992.

[41] S. Chen, M. Zhang, X. Shao, X. Wang, L. Zhang, P. Xu, W. Zhong, L. Zhang, M. Xing, and L. Zhang, "A laminin mimetic peptide SIKVAV-conjugated chitosan hydrogel promoting wound healing by enhancing angiogenesis, re-epithelialization and collagen deposition," *J. Mater. Chem. B*, vol. 3, no. 33, pp. 6798–6804, 2015.

[42] M. C. Kibbey, M. L. Corcoran, L. M. Wahl, and H. K. Kleinman, "Laminin SIKVAV peptide-induced angiogenesis in vivo is potentiated by neutrophils," *J. Cell. Physiol.*, vol. 160, no. 1, pp. 185–193, 1994.

[43] R. Suedee, C. Bodhibukkana, N. Tangthong, C. Amnuaikit, S.

Kaewnopparat, and T. Srichana, “Development of a reservoir-type transdermal enantioselective-controlled delivery system for racemic propranolol using a molecularly imprinted polymer composite membrane,” *J. Control. Release*, vol. 129, no. 3, pp. 170–178, 2008.

[44] E. Trovatti, C. S. R. Freire, P. C. Pinto, I. F. Almeida, P. Costa, A. J. D. Silvestre, C. P. Neto, and C. Rosado, “Bacterial cellulose membranes applied in topical and transdermal delivery of lidocaine hydrochloride and ibuprofen: In vitro diffusion studies,” *Int. J. Pharm.*, vol. 435, no. 1, pp. 83–87, 2012.

[45] C. Bodhibukkana, T. Srichana, S. Kaewnopparat, N. Tangthong, P. Bouking, G. P. Martin, and R. Suedee, “Composite membrane of bacterially-derived cellulose and molecularly imprinted polymer for use as a transdermal enantioselective controlled-release system of racemic propranolol,” *J. Control. Release*, vol. 113, no. 1, pp. 43–56, 2006.

[46] V. Kumar and T. Yang, “HNO3/H3PO4-NANO2 mediated oxidation of cellulose - Preparation and characterization of bioabsorbable oxidized celluloses in high yields and with different levels of oxidation,” *Carbohydr. Polym.*, vol. 48, no. 4, pp. 403–412, 2002.

[47] T. Y. Liu, W. C. Lin, L. Y. Huang, S. Y. Chen, and M. C. Yang, “Hemocompatibility and anaphylatoxin formation of protein-immobilizing polyacrylonitrile hemodialysis membrane,” *Biomaterials*, vol. 26, no. 12, pp. 1437–1444, 2005.

[48] S. Moore, “Amino acid analysis: aqueous dimethyl sulfoxide as solvent for the ninhydrin reaction.,” *J. Biol. Chem.*, vol. 243, no. 23, pp. 6281–6283, 1968.

[49] International Organization for Standardization, “Biological Evaluation of Medical Devices Part 5: Tests for In Vitro Cytotoxicity,” *Iso 10993–5.*, vol. 5, pp. 1 – 52, 2009.

[50] Y. Z. Wan, Y. Huang, C. D. Yuan, S. Raman, Y. Zhu, H. J. Jiang, F. He, and C. Gao, “Biomimetic synthesis of hydroxyapatite/bacterial cellulose nanocomposites for biomedical applications,” *Mater. Sci. Eng. C*, vol. 27, no. 4, pp. 855–864, 2007.

[51] X. Wen, Y. Zheng, J. Wu, L. N. Wang, Z. Yuan, J. Peng, and H.

Meng, “Immobilization of collagen peptide on dialdehyde bacterial cellulose nanofibers via covalent bonds for tissue engineering and regeneration,” *Int. J. Nanomedicine*, vol. 10, pp. 4623–4637, 2015.

[52] W. K. Czaja, D. J. Young, M. Kawecki, and R. M. Brown, “The future prospects of microbial cellulose in biomedical applications,” *Biomacromolecules*, vol. 8, no. 1. pp. 1–12, 2007.

[53] P. Friedl, “Prespecification and plasticity: Shifting mechanisms of cell migration,” *Current Opinion in Cell Biology*, vol. 16, no. 1. pp. 14–23, 2004.

[54] D. Herrmann, J. R. W. Conway, C. Vennin, A. Magenau, W. G. Hughes, J. P. Morton, and P. Timpson, “Three-dimensional cancer models mimic cell-matrix interactions in the tumour microenvironment,” *Carcinogenesis*, vol. 35, no. 8, 2014.

[55] B. Vogelstein and K. W. Kinzler, “Cancer genes and the pathways they control,” *Nat. Med.*, vol. 10, no. 8, pp. 789–799, 2004.

[56] D. Hanahan and R. A. Weinberg, “Hallmarks of cancer: The next generation,” *Cell*, vol. 144, no. 5. pp. 646–674, 2011.

[57] K. M. Yamada and E. Cukierman, “Modeling Tissue Morphogenesis and Cancer in 3D,” *Cell*, vol. 130, no. 4. pp. 601–610, 2007.

[58] R. Pertile, S. Moreira, F. Andrade, L. Domingues, and M. Gama, “Bacterial cellulose modified using recombinant proteins to improve neuronal and mesenchymal cell adhesion,” *Biotechnol. Prog.*, vol. 28, no. 2, pp. 526–532, 2012.

[59] C. S. Szot, C. F. Buchanan, P. Gatenholm, M. N. Rylander, and J. W. Freeman, “Investigation of cancer cell behavior on nanofibrous scaffolds,” *Mater. Sci. Eng. C*, vol. 31, no. 1, pp. 37–42, 2011.

[60] F. J. O’Brien, B. A. Harley, I. V. Yannas, and L. J. Gibson, “The effect of pore size on cell adhesion in collagen-GAG scaffolds,” *Biomaterials*, vol. 26, no. 4, pp. 433–441, 2005.

[61] J. Zeltinger, J. K. Sherwood, D. a Graham, R. Müeller, and L. G. Griffith, “Effect of Pore Size and Void Fraction on Cellular Adhesion, Proliferation, and Matrix Deposition,” *Tissue Eng.*, vol. 7, no. 5, pp. 557–572, 2001.

[62] S. Yang, K. F. Leong, Z. Du, and C. K. Chua, “The design of scaffolds for use in tissue engineering. Part I. Traditional factors.,” *Tissue Eng.*, vol. 7, no. 6, pp. 679–89, 2001.

[63] J. Weber and L. Bergström, “Mesoporous hydrogels: Revealing reversible porosity by cryoporometry, X-ray scattering, and gas adsorption,” *Langmuir*, vol. 26, no. 12, pp. 10158–10164, 2010.

[64] J. F. Godinho, F. V. Berti, D. M??ller, C. R. Rambo, and L. M. Porto, “Incorporation of Aloe vera extracts into nanocellulose during biosynthesis,” *Cellulose*, vol. 23, no. 1, pp. 545–555, 2016.

[65] J. Guo and J. M. Catchmark, “Surface area and porosity of acid hydrolyzed cellulose nanowhiskers and cellulose produced by Gluconacetobacter xylinus,” *Carbohydr. Polym.*, vol. 87, no. 2, pp. 1026–1037, 2012.

[66] H. G. Oliveira Barud, H. D. S. Barud, M. Cavicchioli, T. S. Do Amaral, O. B. De Oliveira Junior, D. M. Santos, A. L. De Oliveira Almeida Petersen, F. Celes, V. M. Borges, C. I. De Oliveira, P. F. De Oliveira, R. A. Furtado, D. C. Tavares, and S. J. L. Ribeiro, “Preparation and characterization of a bacterial cellulose/silk fibroin sponge scaffold for tissue regeneration,” *Carbohydr. Polym.*, vol. 128, pp. 41–51, 2015.

[67] C. W. Kim, D. S. Kim, S. Y. Kang, M. Marquez, and Y. L. Joo, “Structural studies of electrospun cellulose nanofibers,” *Polymer (Guildf).*, vol. 47, no. 14, pp. 5097–5107, 2006.

[68] H. Stopper, S. O. Mueller, and W. K. Lutz, “Supra-additive genotoxicity of a combination of gamma-irradiation and ethyl methanesulfonate in mouse lymphoma L5178Y cells.,” *Mutagenesis*, vol. 15, no. 3, pp. 235–8, 2000.

[69] F. Fehlauer, M. Muench, D. Rades, L. J. A. Stalpers, S. Leenstra, P. Van Der Valk, B. Slotman, E. J. Smid, and P. Sminia, “Effects of irradiation and cisplatin on human glioma spheroids: Inhibition of cell proliferation and cell migration,” *J. Cancer Res. Clin. Oncol.*, vol. 131, no. 11, pp. 723–732, 2005.

[70] A. Ivascu and M. Kubbies, “Rapid generation of single-tumor spheroids for high-throughput cell function and toxicity analysis,” *J Biomol Screen*, vol. 11, no. 8, pp. 922–932, 2006.

[71] R. A. Francescone III, M. Faibish, and R. Shao, “A Matrigel-

Based Tube Formation Assay to Assess the Vasculogenic Activity of Tumor Cells," *Journal of Visualized Experiments*, no. 55. 2011.

[72] Y. Kikkawa, K. Hozumi, F. Katagiri, M. Nomizu, H. K. Kleinman, and J. E. Koblinski, "Laminin-111-derived peptides and cancer," *Cell Adhesion and Migration*, vol. 7, no. 1. pp. 150–159, 2013.

[73] Y. Assal, M. Mie, and E. Kobatake, "The promotion of angiogenesis by growth factors integrated with ECM proteins through coiled-coil structures," *Biomaterials*, vol. 34, no. 13, pp. 3315–3323, 2013.

[74] M. Nakamura, M. Mie, H. Mihara, M. Nakamura, and E. Kobatake, "Construction of multi-functional extracellular matrix proteins that promote tube formation of endothelial cells," *Biomaterials*, vol. 29, no. 20, pp. 2977–2986, 2008.

[75] K. Tashiro, G. C. Sephel, B. Weeks, M. Sasaki, G. R. Martin, H. K. Kleinman, and Y. Yamada, "A synthetic peptide containing the IKVAV sequence from the A chain of laminin mediates cell attachment, migration, and neurite outgrowth," *J. Biol. Chem.*, vol. 264, no. 27, pp. 16174–16182, 1989.

5 CONCLUSÕES GERAIS

A nanocelulose bacteriana é um biomaterial amplamente utilizado na área biomédica e engenharia de tecidos, devido suas propriedades e sua biocompatibilidade. Entretanto, pouco se tem explorado o uso deste material como plataforma para estudo do comportamento de células tumorais. Neste trabalho foram desenvolvidos biomateriais a base de nanocelulose bacteriana para mimetização do microambiente tumoral, afim de se criar plataformas que possam servir como triagem de fármacos na angiogênese e no mimetismo vasculogênico.

Em síntese, podemos concluir que:

A funcionalização dos hidrogéis de nanocelulose bacteriana com heparina e IKVAV foi realizada com sucesso. A imobilização dessas moléculas na superfície dos hidrogéis foi confirmada e os biomateriais sintetizados não apresentaram citotoxicidade.

As células cultivas sobre os hidrogéis sintetizados (BNC-HEP e BNC-IKVAV) mostraram comportamentos dependentes da funcionalização e da estrutura dos biomateriais.

BNC-HEP mostrou aumentar a adesão e proliferação de células endoteliais de veia umbilical humana (HUVECs). Além disso, o lado inferior do hidrogel BNC-HEP foi capaz de induzir a tubulogênese em HUVECs. Assim, BNC-HEP pode ser utilizada como plataforma para testes iniciais da angiogênese, como adesão, proliferação e tubulogênese, com a vantagem da interferência de apenas um tipo de molécula sinalizadora no biomaterial, heparina.

BNC-IKVAV foi capaz de induzir várias plasticidades celulares em células de melanoma humano, SK-MEL-28. Quando essas células foram cultivadas sobre as plataformas BNC-IKVAV aumentaram a adesão e proliferação, comparadas ao hidrogel puro de BNC. Tumoroides foram formados quando células SK-MEL-28 foram semeadas sobre o hidrogel BNC puro. No lado superior de BNC-IKVAV as células invasivas de melanoma apresentaram plasticidades características do processo de migração na metástase. O lado inferior de

BNC-IKVAV induziu mimetismo vasculogênico após 24 horas de cultura de SK-MEL-28.

As plataformas desenvolvidas podem ser potencialmente utilizadas para superar as limitações das plataformas atuais em testes de triagem de fármacos para inibir a angiogênese, mimetismo vasculogênico e outras plasticidades tumorais Além disso, BNC, BNC-HEP e BNC-IKVAV podem ser utilizadas como plataformas de estudo do comportamento celular.

6 REFERÊNCIAS

ADAIR, T. H.; MONTANI, J.-P. Angiogenesis in Granger DN, Granger JP (eds): Integrated Systems Physiology: from Molecule to Function to Disease. Morgan & Claypool Life Sciences, v. 2, p. 1–84, 2010.

ASGHAR, W. et al. Engineering cancer microenvironments for in vitro 3-D tumor modelsMaterials Today, v. 18, n.10, p. 539–553, 2015.

ASSAL, Y.; MIE, M.; KOBATAKE, E. The promotion of angiogenesis by growth factors integrated with ECM proteins through coiled-coil structures. Biomaterials, v. 34, n. 13, p. 3315–3323, 2013.

BALTIĆ, V. Sentinel-node biopsy or nodal observation in melanomaArchive of Oncology, v. 355, n. 13, p. 1307–1317, 2006.

BERTI, F. V. et al. Nanofiber density determines endothelial cell behavior on hydrogel matrix. Materials Science and Engineering C, v. 33, n. 8, p. 4684–4691, 2013.

BISSELL, M. J.; RADISKY, D. Putting tumours in context. Nature reviews. Cancer, v. 1, n. 1, p. 46–54, 2001.

BODHIBUKKANA, C. et al. Composite membrane of bacterially-derived cellulose and molecularly imprinted polymer for use as a transdermal enantioselective controlled-release system of racemic propranolol. Journal of Controlled Release, v. 113, n. 1, p. 43–56, 2006.

BOND, J. H. Colon polyps and cancer. Endoscopy, v. 37, n. 3, p. 208–212, 2005.

BROWN, E. E.; LABORIE, M. P. G.; ZHANG, J. Glutaraldehyde treatment of bacterial cellulose/fibrin composites: Impact on

morphology, tensile and viscoelastic properties. Cellulose, v. 19, n. 1, p. 127–137, 2012.

CAPILA, I.; LINHARDT, R. J. Heparin-protein interactions. Angewandte Chemie (International ed. in English), v. 41, n. 3, p. 391–412, 2002.

CARMELIET, P.; JAIN, R. K. Angiogenesis in cancer and other diseases. Nature, v. 407, n. 6801, p. 249–257, 2000.

CHAFFER, C. L.; WEINBERG, R. A. A perspective on cancer cell metastasis. Science (New York, N.Y.), v. 331, n. 6024, p. 1559–1564, 2011.

COLLA, G.; PORTO, L. Development of artificial blood vessels through tissue engineering. BMC Proceedings, v. 8, n. 4, p. P45, 2014.

CZAJA, W. K. et al. The future prospects of microbial cellulose in biomedical applicationsBiomacromolecules, v.8, n. 1, p. 1–12, 2007.

DAVIS, G. E.; SAUNDERS, W. B. Molecular balance of capillary tube formation versus regression in wound repair: role of matrix metalloproteinases and their inhibitors. The journal of investigative dermatology Symposium proceedings the Society for Investigative Dermatology Inc and European Society for Dermatological Research, v. 11, n. 1, p. 44–56, 2006.

DE SMET, F. et al. Mechanisms of vessel branching: Filopodia on endothelial tip cells lead the wayArteriosclerosis, Thrombosis, and Vascular Biology, v. 29, n. 5, p. 639-649, 2009.

DEBNATH, J.; BRUGGE, J. S. Modelling glandular epithelial cancers in three-dimensional cultures. Nature reviews. Cancer, v. 5, n. 9, p. 675–88, 2005.

DÖME, B. et al. Alternative vascularization mechanisms in cancer: Pathology and therapeutic implications. The American journal of pathology, v. 170, n. 1, p. 1–15, 2007.

DRURY, J. L.; MOONEY, D. J. Hydrogels for tissue engineering: Scaffold design variables and applicationsBiomaterials, v. 24, n. 24, p. 4337-4351, 2003.

EL-SHERBINY, I. M.; YACOUB, M. H. Hydrogel scaffolds for tissue engineering: Progress and challenges. Global Cardiology Science and Practice, v. 2013, n. 3, p. 38, 2013.

EL-SHERBINY, I.; YACOUB, M. Hydrogel scaffolds for tissue engineering: Progress and challenges. Global cardiology science & practice, v. 2013, n. 3, p. 316–42, 2013b.

FOLBERG, R.; HENDRIX, M. J.; MANIOTIS, A J. Vasculogenic mimicry and tumor angiogenesis. The American journal of pathology, v. 156, n. 2, p. 361–381, 2000.

FOLBERG, R.; MANIOTIS, A. J. Vasculogenic mimicry. APMIS, v. 112, n. 7-8, p. 508-525, 2004.

FOLKMAN, J. Tumor angiogenesis: therapeutic implications. The New England journal of medicine, v. 285, n. 21, p. 1182–1186, 1971.

FRIEDL, P. Prespecification and plasticity: Shifting mechanisms of cell migration. Current Opinion in Cell Biology, v. 16, n. 1, p. 14-23, 2004.

FRIEDL, P.; ALEXANDER, S. Cancer invasion and the microenvironment: Plasticity and reciprocity. Cell, v. 147, n. 5, p. 992-1009, 2011.

FRIEDL, P.; WOLF, K. Tumour-cell invasion and migration: diversity and escape mechanisms. Nature reviews. Cancer, v. 3, n. 5, p. 362–74, 2003.

GEIGER, T. R.; PEEPER, D. S. Metastasis mechanisms. Biochimica et Biophysica Acta - Reviews on Cancer, v. 1796, n. 2, p. 293-308, 2009.

GEVAERT, M. Engineering 3D Tissue Systems to Better Mimic Human Biology. In: The bridge: Linking Engineering and Society. v. 42p. 48–55.

GRANT, D. S. et al. Interaction of endothelial cells with a laminin A chain peptide (SIKVAV) in vitro and induction of angiogenic behavior in vivo. Journal of cellular physiology, v. 153, n. 3, p. 614–25, 1992.

HAIT, W. N. Anticancer drug development: the grand challenges. Nature reviews. Drug discovery, v. 9, n. 4, p. 253–254, 2010.

HANAHAN, D.; WEINBERG, R. A. Hallmarks of cancer: The next generation. Cell, v. 144, n. 5, p. 646-674, 2011.

HEJMADI, M. Introduction to Cancer Biology. Bookboon, London, 2010.

HENDRIX, M. J. C. et al. Vasculogenic mimicry and tumour-cell plasticity: lessons from melanoma. Nature reviews. Cancer, v. 3, n. 6, p. 411–21, 2003.

HENDRIX, M. J. C. et al. Tumor cell vascular mimicry: Novel targeting opportunity in melanoma. Pharmacology and Therapeutics, v. 159, p. 83-92, 2016.

HOSSEINKHANI, H. et al. Engineering three-dimensional collagen-IKVAV matrix to mimic neural microenvironment. ACS Chemical Neuroscience, v. 4, n. 8, p. 1229–1235, 2013.

HUGHES, C. S.; POSTOVIT, L. M.; LAJOIE, G. A. Matrigel: a complex protein mixture required for optimal growth of cell culture. Proteomics, v. 10, n. 9, p. 1886–1890, 2010.

HULKOWER, K. I.; HERBER, R. L. Cell migration and invasion assays as tools for drug discovery. Pharmaceutics, v. 3, n. 1, p. 107-124, 2011.

INSTITUTO NACIONAL DE CANCER JOSÉ ALENCAR GOMES DA SILVA. INCA - Instituto Nacional de Câncer - Estimativa 2016. [s.l: s.n.].

JAIN, R. K. Delivery of molecular and cellular medicine to solid tumors. Advanced Drug Delivery Reviews, ;v. 46, n. 1-3, p. 149-168, 2012.

JOYCE, J. A; POLLARD, J. W. Microenvironmental regulation of metastasis. Nature Reviews Cancer, v. 9, n. 4, p. 239–252, 2009.

KHALIL, A. A; FRIEDL, P. Determinants of leader cells in collective cell migration. Integrative biology : quantitative biosciences from nano to macro, v. 2, n. 11-12, p. 568–574, 2010.

KIBBEY, M. C. et al. Laminin SIKVAV peptide-induced angiogenesis in vivo is potentiated by neutrophils. Journal of Cellular Physiology, v. 160, n. 1, p. 185–193, 1994.

KIMLIN, L. C.; CASAGRANDE, G.; VIRADOR, V. M. In vitro three-dimensional (3D) models in cancer research: an update. Mol Carcinog, v. 52, n. 3, p. 167–182, 2013a.

KIMLIN, L. C.; CASAGRANDE, G.; VIRADOR, V. M. In vitro three-dimensional (3D) models in cancer research: An update. Molecular Carcinogenesis, v. 52, n. 3, p. 167–182, 2013b.

KLEINMAN, H. K.; MARTIN, G. R. Matrigel: Basement membrane matrix with biological activity. Seminars in Cancer Biology, v. 15, n. 5 SPEC. ISS., p. 378–386, 2005.

KLEMM, D. et al. Bacterial synthesized cellulose - Artificial blood vessels for microsurgery. Progress in Polymer Science (Oxford), v. 26, n. 9, p. 1561–1603, 2001.

KLEMM, D. et al. Nanocelluloses: A new family of nature-based materials. Angewandte Chemie - International Edition, v. 50, n. 24, p. 5438–54662011, 2011.

KULAR, J. K.; BASU, S.; SHARMA, R. I. The extracellular matrix: Structure, composition, age-related differences, tools for analysis and applications for tissue engineering. Journal of tissue engineering, v. 5, p. 1–17, 2014.

LÄMMERMANN, T.; SIXT, M. Mechanical modes of “amoeboid” cell migration. Current Opinion in Cell Biology, v. 21, n. 5, p. 636-644, 2009.

LARSON, A. R. et al. Melanoma spheroid formation involves laminin-associated vasculogenic mimicry. American Journal of Pathology, v. 184, n. 1, p. 71–78, 2014.

LIANG, Y. et al. A cell-instructive hydrogel to regulate malignancy of 3D tumor spheroids with matrix rigidity. Biomaterials, v. 32, n. 35, p. 9308–9315, 2011.

LIGHT, D. W.; KANTARJIAN, H. Market spiral pricing of cancer drugs. Cancer, v. 119, p. :3900-2, 2013.

MANIOTIS, A. J. et al. Vascular channel formation by human melanoma cells in vivo and in vitro: vasculogenic mimicry. Am J Pathol, v. 155, n. 3, p. 739–752, 1999a.

MANIOTIS, A. J. et al. Vascular channel formation by human melanoma cells in vivo and in vitro: vasculogenic mimicry. Am.J.Pathol., v. 155, n. 3, p. 739–752, 1999b.

MARTIN, T. A. et al. Cancer Invasion and Metastasis: Molecular and Cellular Perspective. Disponível em: <http://www.ncbi.nlm.nih.gov/books/NBK164700/?report=classic>. MATSUOKA, T.; YASHIRO, M. Rho/ROCK signaling in motility and metastasis of gastric cancerWorld Journal of Gastroenterology, 2014.

MILLER, J. S. et al. Bioactive hydrogels made from step-growth derived PEG-peptide macromers. Biomaterials, v. 31, n. 13, p. 3736–3743, 2010.

MITCH LESLIE. Tumors have found a bloody new way to grow and spread. Disponível em: <http://www.sciencemag.org/news/2016/06/tumors-have-found-bloody-new-way-grow-and-spread?utm_source=sciencemagazine&utm_medium=facebook-text&utm_campaign=bloodytumor-5059>. Acesso em: 10 jul. 2016.

NGUYEN, D. X.; BOS, P. D.; MASSAGUÉ, J. Metastasis: from dissemination to organ-specific colonization. Nature reviews. Cancer, v. 9, n. 4, p. 274–284, 2009.

NGUYEN, K. T.; WEST, J. L. Photopolymerizable hydrogels for tissue engineering applications. Biomaterials, v. 23, n. 22, p. 4307–4314, 2002.

NYGA, A.; CHEEMA, U.; LOIZIDOU, M. 3D tumour models: Novel in vitro approaches to cancer studies. Journal of Cell Communication and Signaling, v. 5, n. 3, p. 239-248, 2011.

OU, K.-L.; HOSSEINKHANI, H. Development of 3D in Vitro Technology for Medical Applications. International Journal of Molecular Sciences, v. 15, n. 10, p. 17938–17962, 2014.

P??RTILE, R. et al. Bacterial cellulose modified using recombinant proteins to improve neuronal and mesenchymal cell adhesion. Biotechnology Progress, v. 28, n. 2, p. 526–532, 2012.

PARK, J.; PARK, Y.; JUNG, J. Production of bacterial cellulose byGluconacetobacter hansenii PJK isolated from rotten apple. Biotechnology and Bioprocess Engineering, v. 8, p. 83 – 88, 2003.

PASSALIDOU, E. et al. Vascular phenotype in angiogenic and non-angiogenic lung non-small cell carcinomas. British journal of cancer, v. 86, n. 2, p. 244–249, 2002.

PAULIS, Y. W. J. et al. Signalling pathways in vasculogenic mimicry. Biochimica et Biophysica Acta - Reviews on Cancer, v. 1806, n. 1, p.18-28, 2010.

PEPPAS, N. A. et al. Hydrogels in biology and medicine: From molecular principles to bionanotechnology. Advanced Materials, v. 18, n. 11, p. 1345–1360, 2006.

QIAO, L. et al. Advanced research on vasculogenic mimicry in cancer. Journal of Cellular and Molecular Medicine, v. 19, n. 2, p. 315–326, 2015.

RAJANGAM, K. et al. Heparin binding nanostructures to promote growth of blood vessels. Nano Letters, v. 6, n. 9, p. 2086–2090, 2006.

RAMBO, C. R. et al. Template assisted synthesis of porous nanofibrous cellulose membranes for tissue engineering. Materials Science and Engineering C, v. 28, n. 4, p. 549–554, 2008.

RECOUVREUX, D. O. S. et al. Novel three-dimensional cocoon-like hydrogels for soft tissue regeneration. Materials Science and Engineering C, v. 31, n. 2, p. 151–157, 2011.

RHODES, J. M.; SIMONS, M. The extracellular matrix and blood vessel formation: not just a scaffold. Journal of cellular and molecular medicine, v. 11, n. 2, p. 176–205, 2007.

RISAU, W. Mechanisms of angiogenesis.Nature, v. 38, n. 6626, p. 671-4, 1997.

SAMOLOV, B. et al. Delayed inflammation-associated corneal neovascularization in MMP-2-deficient mice. Experimental Eye Research, v. 80, n. 2, p. 159–166, 2005.

SHIRAKAWA, K. et al. Absence of endothelial cells, central necrosis, and fibrosis are associated with aggressive inflammatory breast cancer. Cancer Res, v. 61, n. 2, p. 445–451, 2001.

SHOJAEI, F. Anti-angiogenesis therapy in cancer: Current challenges and future perspectives. Cancer Letters, v. 320, n. 2, p. 130-7, 2012.

SOOD, A K. et al. Molecular determinants of ovarian cancer plasticity. The American journal of pathology, v. 158, n. 4, p. 1279–88, 2001.

STEEN, B. et al. Matrix metalloproteinases and metalloproteinase inhibitors in choroidal neovascular membranes. Investigative Ophthalmology and Visual Science, v. 39, n. 11, p. 2194–2200, 1998.

SUEDEE, R. et al. Development of a reservoir-type transdermal enantioselective-controlled delivery system for racemic propranolol using a molecularly imprinted polymer composite membrane. Journal of Controlled Release, v. 129, n. 3, p. 170–178, 2008.

TAN, H.; MARRA, K. G. Injectable, biodegradable hydrogels for tissue engineering applications. Materials, v. 3, n. 3, p. 1746–1767, 2010.

TROVATTI, E. et al. Bacterial cellulose membranes applied in topical and transdermal delivery of lidocaine hydrochloride and ibuprofen: In vitro diffusion studies. International Journal of Pharmaceutics, v. 435, n. 1, p. 83–87, 2012.

TSAI, J. H.; YANG, J. Epithelial-mesenchymal plasticity in carcinoma metastasis. Genes and Development, v. 27, n. 20, p. 2192-1206, 2013.

VALASTYAN, S.; WEINBERG, R. A. Tumor metastasis: Molecular insights and evolving paradigms. Cell, v. 147, n. 2, p. :275-292, 2011.

VAN DER SCHAFT, D. W. J. et al. Effects of angiogenesis inhibitors on vascular network formation by human endothelial and melanoma cells. Journal of the National Cancer Institute, v. 96, n. 19, p. 1473–1477, 2004.

VAN DER SCHAFT, D. W. J. et al. Tumor cell plasticity in Ewing sarcoma, an alternative circulatory system stimulated by hypoxia. Cancer Research, v. 65, n. 24, p. 11520–11528, 2005.

VAN HORSSEN, R.; TEN HAGEN, T. L. M.; EGGERMONT, A. M. M. TNF-α in Cancer Treatment: Molecular Insights, Antitumor Effects, and Clinical Utility. The Oncologist, v. 11, n. 4, p. 397–408, 2006.

VAN VLIERBERGHE, S.; DUBRUEL, P.; SCHACHT, E. Biopolymer-based hydrogels as scaffolds for tissue engineering applications: A reviewBiomacromolecules, 2011.

WAN, L.; PANTEL, K.; KANG, Y. Tumor metastasis: moving new biological insights into the clinic. Nature medicine, v. 19, n. 11, p. 1450–64, 2013.

WOLF, K. et al. Compensation mechanism in tumor cell migration: Mesenchymal-amoeboid transition after blocking of pericellular proteolysis. Journal of Cell Biology, v. 160, n. 2, p. 267–277, 2003.

WOOD, L.; KAMM, R.; ASADA, H. Stochastic modeling and identification of emergent behaviors of an Endothelial Cell population in angiogenic pattern formation. The International Journal of Robotics Research, v. 30, n. 6, p. 659–677, 2011.

WORLD HEALTH ORGANIZATION; STEWART, B. W.; WILD, C. P. World Cancer Report 2014.

YAMADA, K. M.; CUKIERMAN, E. Modeling Tissue Morphogenesis and Cancer in 3D. Cell, v.130, n. 4, p.601-610, 2007.

YAMAGUCHI, H.; WYCKOFF, J.; CONDEELIS, J. Cell migration in tumors. Current Opinion in Cell Biology, v. 17, n. 5, p.559-564, 2005.
ZHIJIANG, C.; GUANG, Y. Bacterial cellulose/collagen composite: Characterization and first evaluation of cytocompatibility. Journal of Applied Polymer Science, v. 120, n. 5, p. 2938–2944, 2011.

ZHU, J.; MARCHANT, R. E. Design properties of hydrogel tissue-engineering scaffolds. Expert review of medical devices, v. 8, n. 5, p. 607–26, 2011.